Efficient Methods of Chaos Detection

Haris Skokos

Max Planck Institute for the Physics of Complex Systems
Dresden, Germany

E-mail: hskokos@pks.mpg.de
URL: http://www.pks.mpg.de/~hskokos/

Outline

- **Hamiltonian systems – Symplectic maps**
  - ✓ **Variational equations**
  - ✓ **Lyapunov exponents**

- **Smaller ALignment Index – SALI**
  - ✓ **Definition**
  - ✓ **Behavior for chaotic and regular motion**
  - ✓ **Applications**

- **Generalized ALignment Index – GALI**
  - ✓ **Definition - Relation to SALI**
  - ✓ **Behavior for chaotic and regular motion**
  - ✓ **Applications**
  - ✓ **Global dynamics**
  - ✓ **Motion on low-dimensional tori**

- **Efficient integration of variational equations**
  - ✓ **The tangent map (TM) method**
  - ✓ **Applications to multidimensional Hamiltonian systems**

- **Conclusions**

Autonomous Hamiltonian systems

Consider an N degree of freedom autonomous Hamiltonian system having a Hamiltonian function of the form:

$$H(\overbrace{q_1,q_2,\ldots,q_N}^{\text{positions}}, \overbrace{p_1,p_2,\ldots,p_N}^{\text{momenta}})$$

The time evolution of an orbit (trajectory) with initial condition

$$P(0)=(q_1(0), q_2(0),\ldots,q_N(0), p_1(0), p_2(0),\ldots,p_N(0))$$

is governed by the Hamilton's equations of motion

$$\frac{dp_i}{dt} = -\frac{\partial H}{\partial q_i} \quad , \quad \frac{dq_i}{dt} = \frac{\partial H}{\partial p_i}$$

Variational Equations

We use the notation $x = (q_1,q_2,\ldots,q_N,p_1,p_2,\ldots,p_N)^T$. The **deviation vector** from a given orbit is denoted by

$$v = (\delta x_1, \delta x_2,\ldots,\delta x_n)^T \text{ , with } n=2N$$

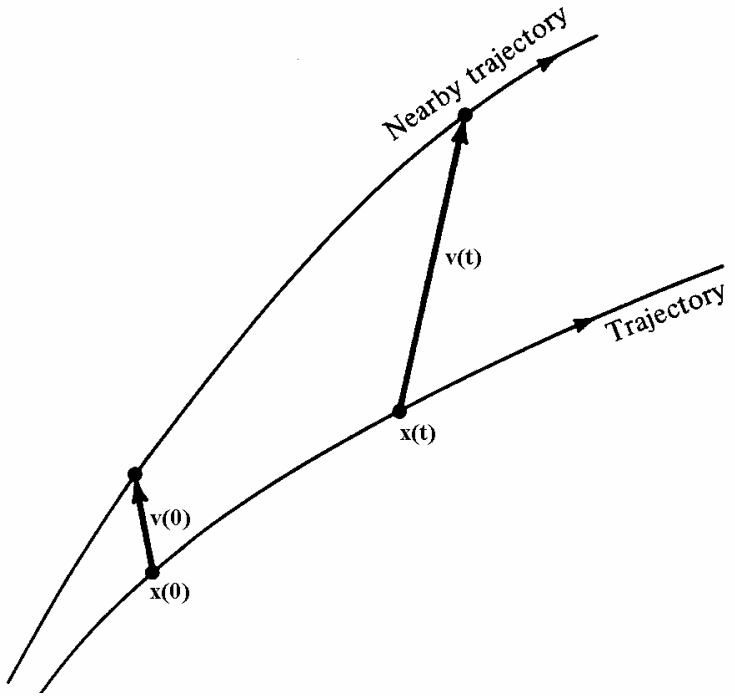

Benettin & Galgani, 1979, in Laval and Gressillon (eds.), op cit, 93

The time evolution of v is given by the so-called **variational equations:**

$$\frac{dv}{dt} = -J \cdot P \cdot v$$

where

$$J = \begin{pmatrix} 0_N & -I_N \\ I_N & 0_N \end{pmatrix}, \quad P_{ij} = \frac{\partial^2 H}{\partial x_i \partial x_j} \quad i,j = 1,2,\ldots,n$$

Symplectic Maps

Consider an 2N-dimensional symplectic map T. In this case we have discrete time.

The evolution of an orbit with initial condition

$$P(0)=(x_1(0), x_2(0),\ldots,x_{2N}(0))$$

is governed by the equations of map T

$$P(i+1)=T\,P(i)\ ,\ i=0,1,2,\ldots$$

The evolution of an initial deviation vector

$$v(0) = (\delta x_1(0), \delta x_2(0),\ldots, \delta x_{2N}(0))$$

is given by the corresponding tangent map

$$v(i+1) = \left.\frac{\partial T}{\partial P}\right|_i \cdot v(i)\ ,\ i = 0,1,2,\ldots$$

Lyapunov Exponents

Roughly speaking, the Lyapunov exponents of a given orbit characterize the mean exponential rate of divergence of trajectories surrounding it.

Consider an orbit in the 2N-dimensional phase space with initial condition x(0) and an initial deviation vector from it v(0). Then the mean exponential rate of divergence is:

$$\sigma(x(0), v(0)) = \lim_{t \to \infty} \frac{1}{t} \ln \frac{\|v(t)\|}{\|v(0)\|}$$

Maximum Lyapunov Exponent

$\sigma_1=0 \rightarrow$ Regular motion

$\sigma_1\neq0 \rightarrow$ Chaotic motion

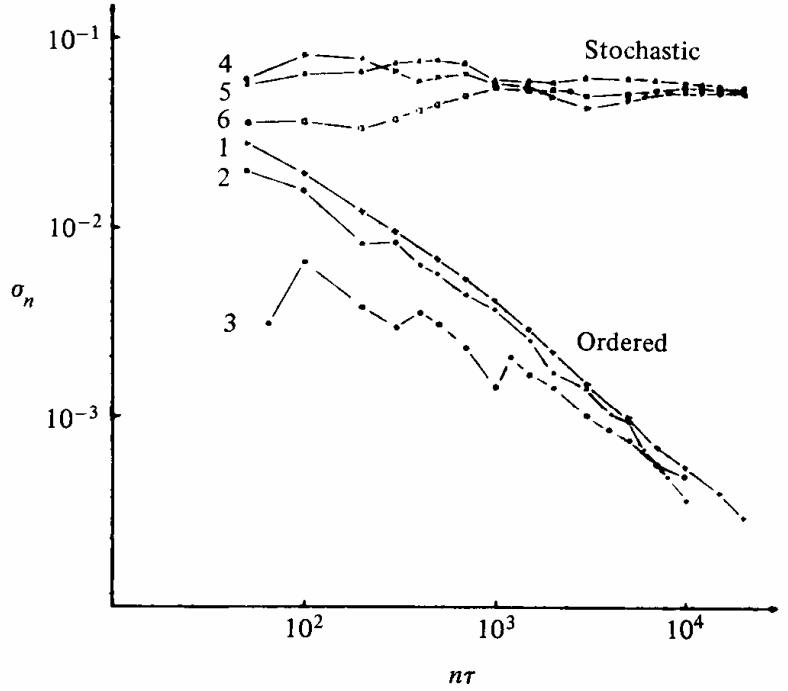

Figure 5.7. Behavior of σ_n at the intermediate energy $E = 0.125$ for initial points taken in the ordered (curves 1–3) or stochastic (curves 4–6) regions (after Benettin *et al.*, 1976).

If we start with more than one linearly independent deviation vectors they will align to the direction defined by the largest Lyapunov exponent for chaotic orbits.

Definition of Smaller Alignment Index (SALI)

Consider the 2N-dimensional phase space of a conservative dynamical system (symplectic map or Hamiltonian flow).

An orbit in that space with initial condition :

$$P(0)=(x_1(0), x_2(0),\ldots,x_{2N}(0))$$

and a deviation vector

$$v(0)=(\delta x_1(0), \delta x_2(0),\ldots, \delta x_{2N}(0))$$

The evolution in time (in maps the time is discrete and is equal to the number n of the iterations) of a deviation vector is defined by:

- **the variational equations (for Hamiltonian flows) and**
- **the equations of the tangent map (for mappings)**

Definition of SALI

We follow the evolution in time of two different initial deviation vectors $(v_1(0), v_2(0))$, and define SALI (Ch.S. 2001, J. Phys. A) as:

$$SALI(t) = \min\left\{\left\|\hat{v}_1(t) + \hat{v}_2(t)\right\|, \left\|\hat{v}_1(t) - \hat{v}_2(t)\right\|\right\}$$

where

$$\hat{v}_1(t) = \frac{v_1(t)}{\left\|v_1(t)\right\|}$$

When the two vectors become collinear

$$SALI(t) \rightarrow 0$$

Behavior of SALI for chaotic motion

For chaotic orbits the two initially different deviation vectors tend to coincide with the direction defined by the maximum Lyapunov exponent.

Behavior of SALI for chaotic motion

For chaotic orbits the two initially different deviation vectors tend to coincide with the direction defined by the maximum Lyapunov exponent.

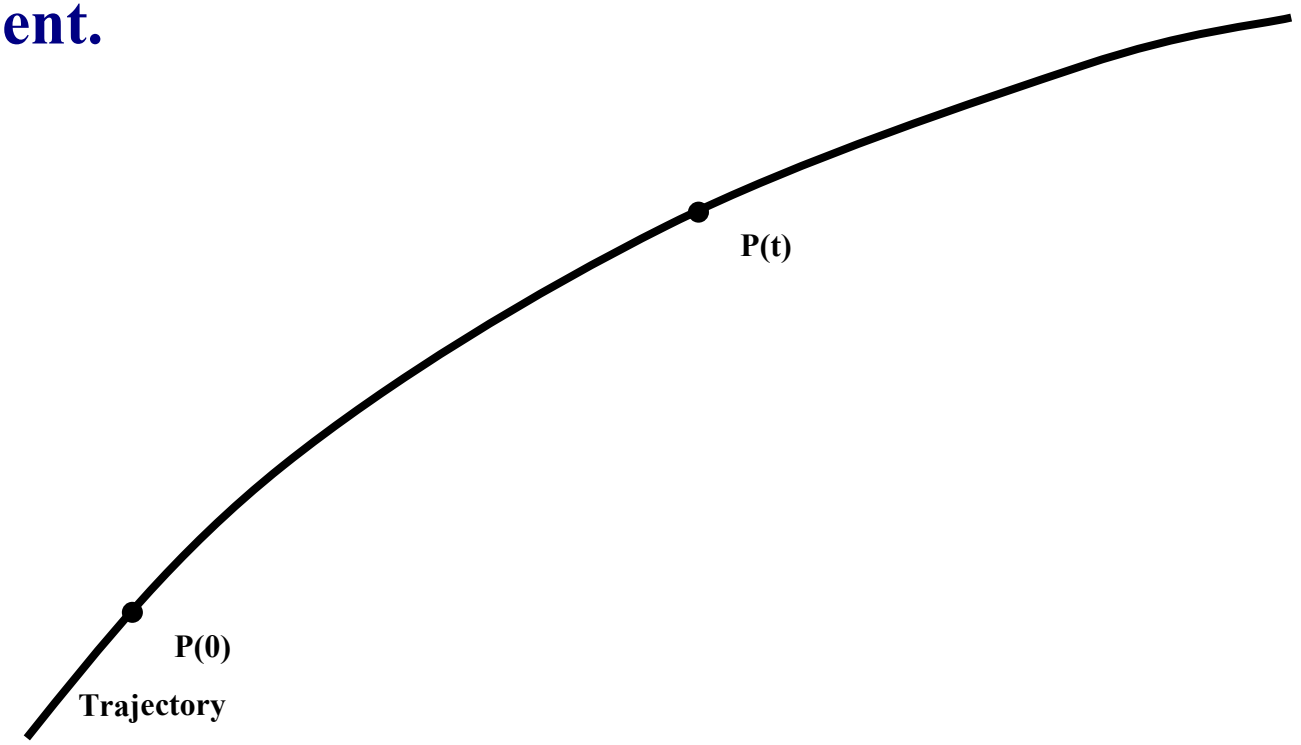

Behavior of SALI for chaotic motion

For chaotic orbits the two initially different deviation vectors tend to coincide with the direction defined by the maximum Lyapunov exponent.

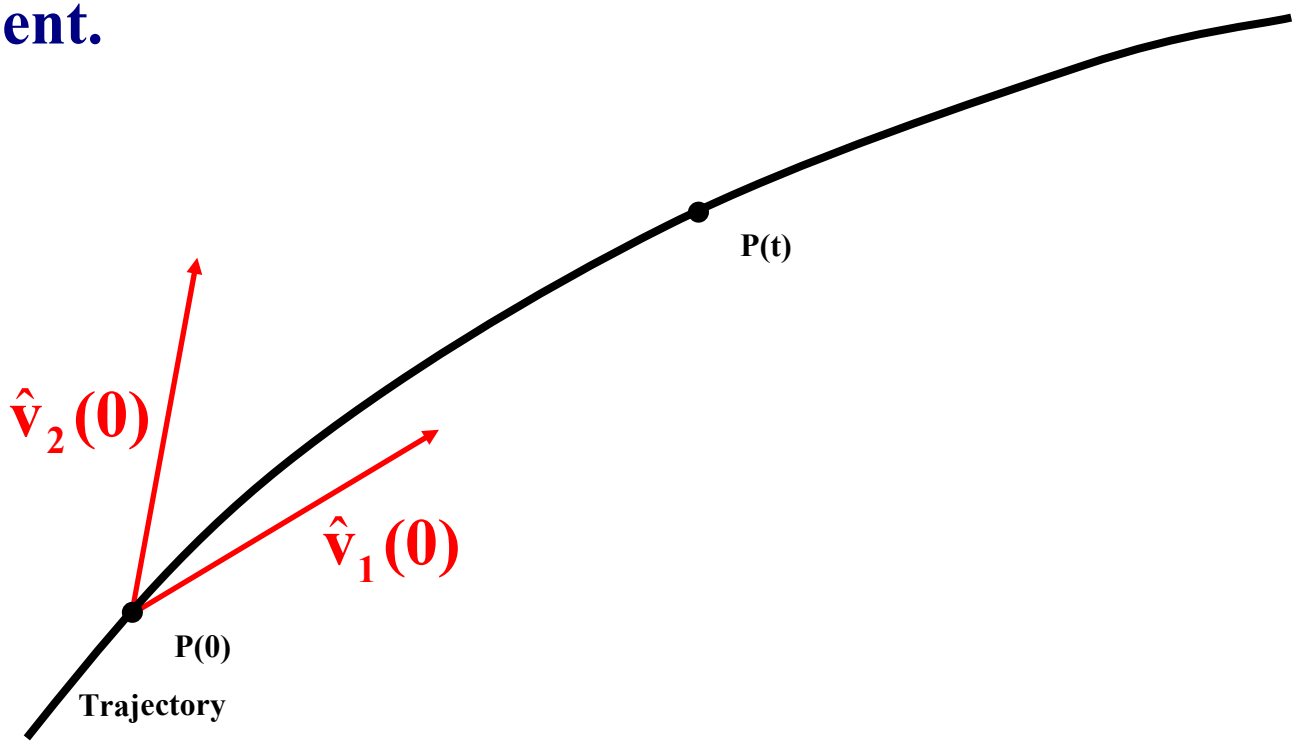

Behavior of SALI for chaotic motion

For chaotic orbits the two initially different deviation vectors tend to coincide with the direction defined by the maximum Lyapunov exponent.

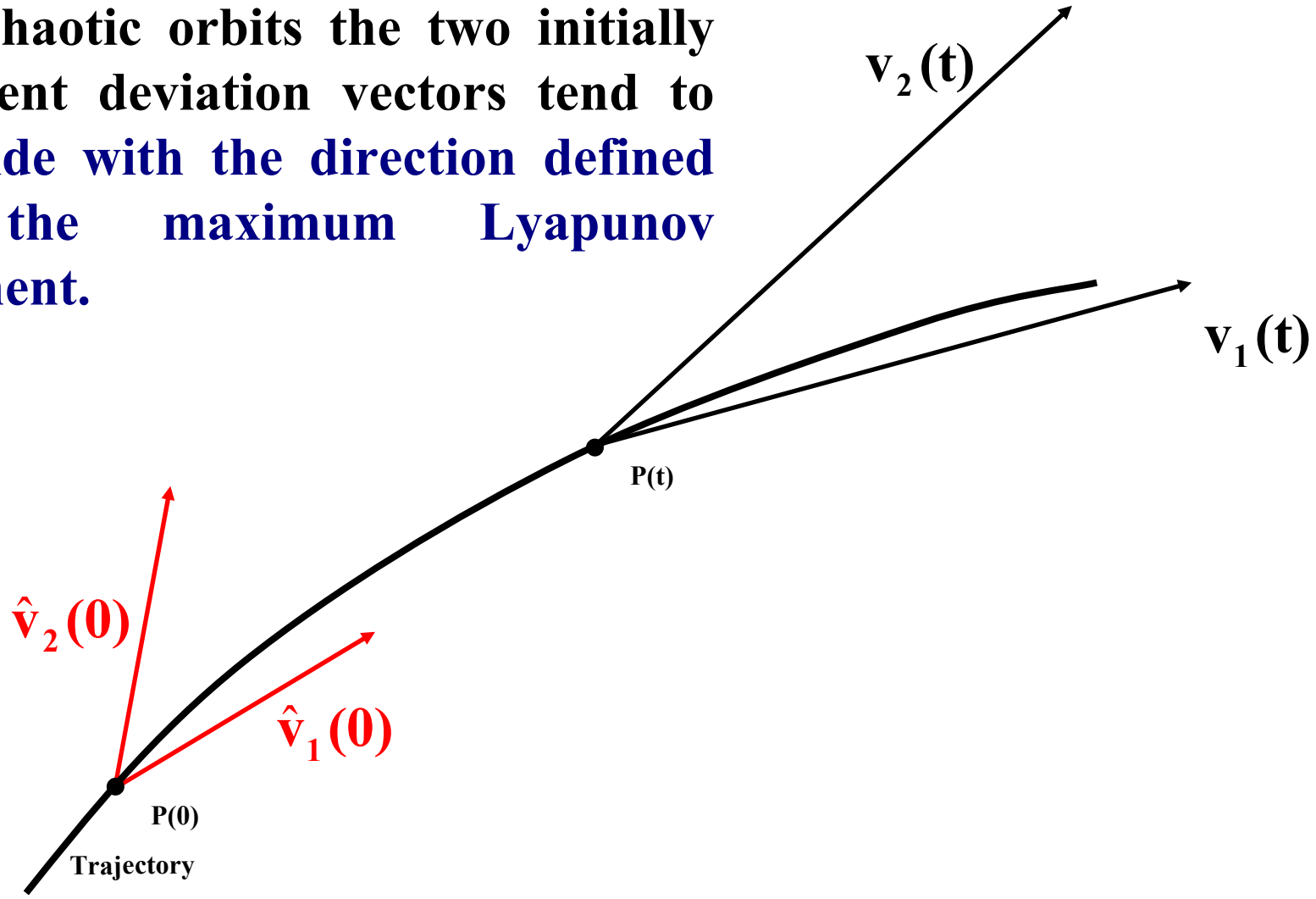

Behavior of SALI for chaotic motion

For chaotic orbits the two initially different deviation vectors tend to coincide with the direction defined by the maximum Lyapunov exponent.

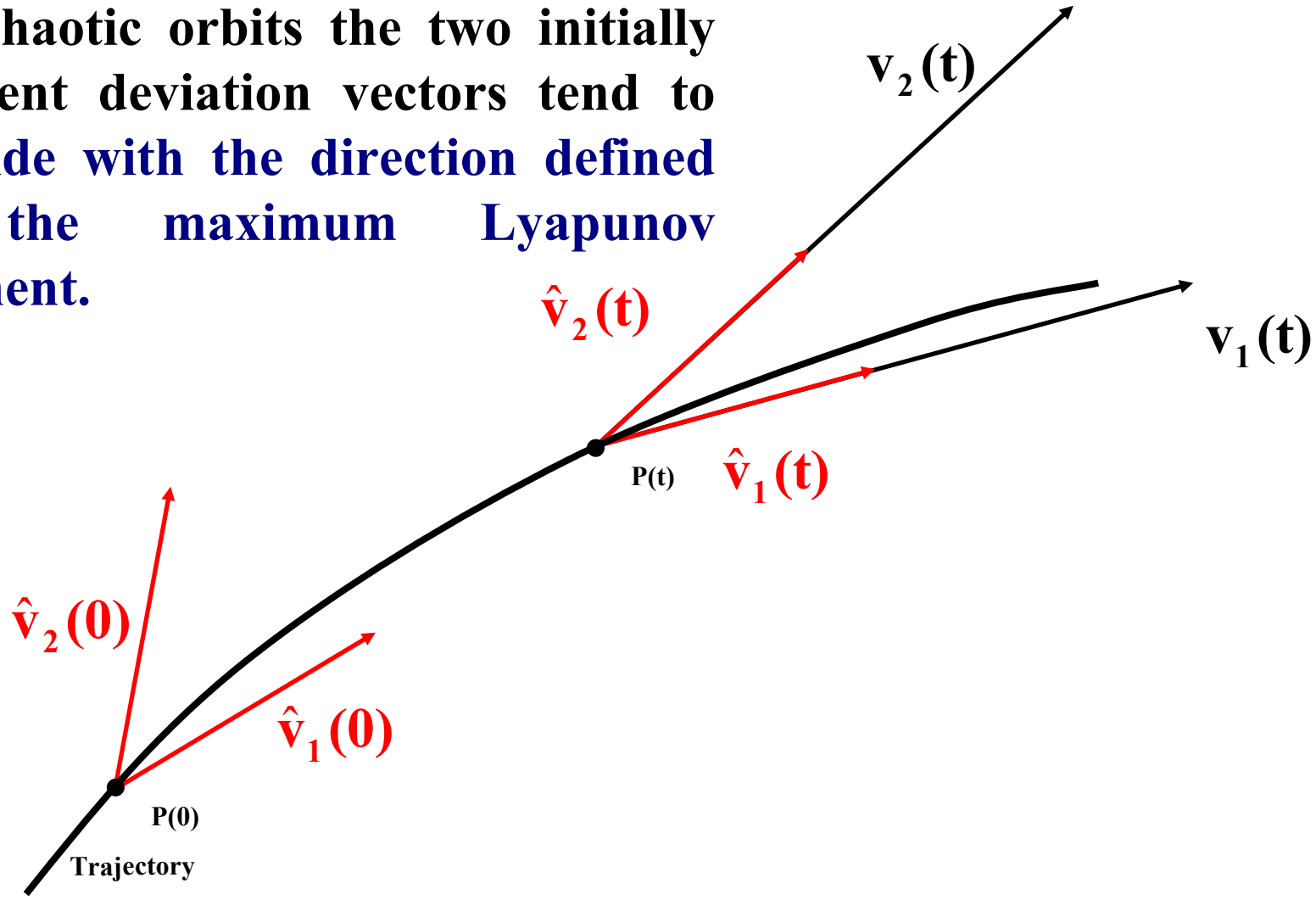

Behavior of SALI for chaotic motion

For chaotic orbits the two initially different deviation vectors tend to coincide with the direction defined by the maximum Lyapunov exponent.

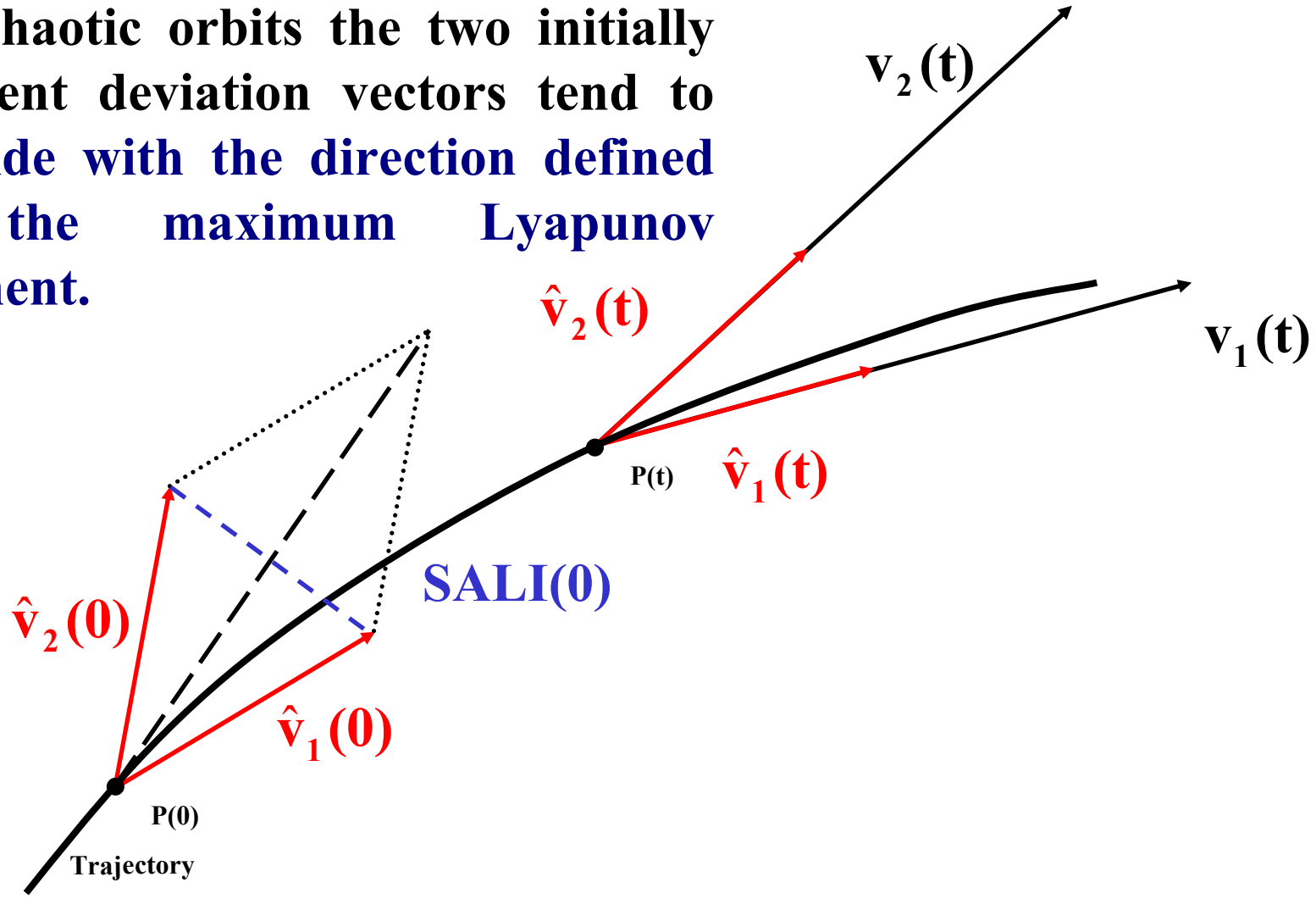

Behavior of SALI for chaotic motion

For chaotic orbits the two initially different deviation vectors tend to coincide with the direction defined by the maximum Lyapunov exponent.

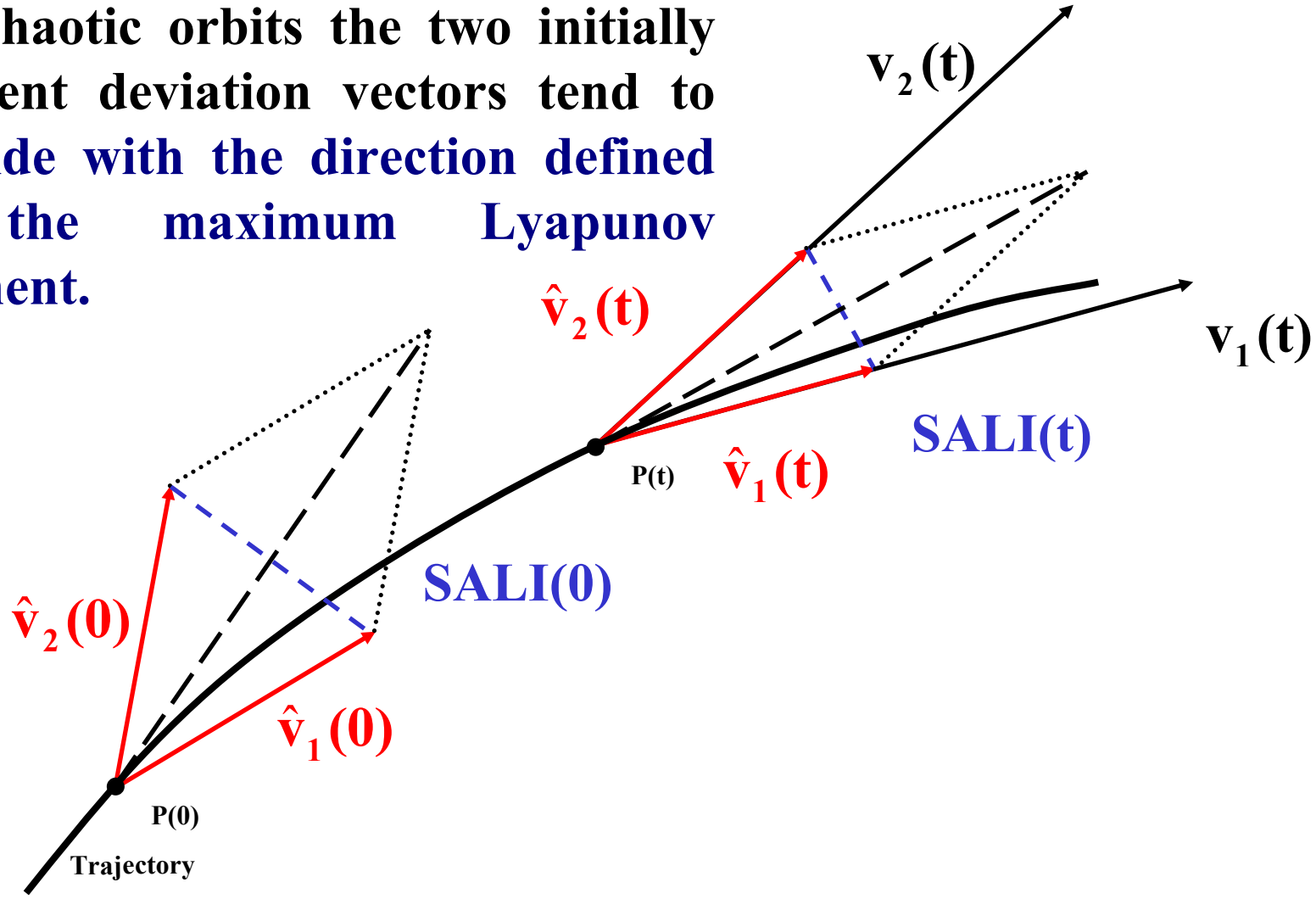

Behavior of SALI for chaotic motion

The evolution of a deviation vector can be approximated by:

$$v_1(t) = \sum_{i=1}^{n} c_i^{(1)} e^{\sigma_i t} \hat{u}_i \approx c_1^{(1)} e^{\sigma_1 t} \hat{u}_1 + c_2^{(1)} e^{\sigma_2 t} \hat{u}_2$$

where $\sigma_1 > \sigma_2 \geq \ldots \geq \sigma_n$ are the Lyapunov exponents. and $\hat{u}_j$ j=1, 2, …, 2N the corresponding eigendirections.

Behavior of SALI for chaotic motion

The evolution of a deviation vector can be approximated by:

$$\mathbf{v}_1(t) = \sum_{i=1}^{n} c_i^{(1)} e^{\sigma_i t} \hat{\mathbf{u}}_i \approx c_1^{(1)} e^{\sigma_1 t} \hat{\mathbf{u}}_1 + c_2^{(1)} e^{\sigma_2 t} \hat{\mathbf{u}}_2$$

where $\sigma_1 > \sigma_2 \geq \ldots \geq \sigma_n$ are the Lyapunov exponents. and $\hat{\mathbf{u}}_j$ j=1, 2, …, 2N the corresponding eigendirections.

In this approximation, we derive a leading order estimate of the ratio

$$\frac{\mathbf{v}_1(t)}{\|\mathbf{v}_1(t)\|} \approx \frac{c_1^{(1)} e^{\sigma_1 t} \hat{\mathbf{u}}_1 + c_2^{(1)} e^{\sigma_2 t} \hat{\mathbf{u}}_2}{\left|c_1^{(1)}\right| e^{\sigma_1 t}} = \pm \hat{\mathbf{u}}_1 + \frac{c_2^{(1)}}{\left|c_1^{(1)}\right|} e^{-(\sigma_1 - \sigma_2)t} \hat{\mathbf{u}}_2$$

and an analogous expression for $\mathbf{v}_2$

$$\frac{\mathbf{v}_2(t)}{\|\mathbf{v}_2(t)\|} \approx \frac{c_1^{(2)} e^{\sigma_1 t} \hat{\mathbf{u}}_1 + c_2^{(2)} e^{\sigma_2 t} \hat{\mathbf{u}}_2}{\left|c_1^{(2)}\right| e^{\sigma_1 t}} = \pm \hat{\mathbf{u}}_1 + \frac{c_2^{(2)}}{\left|c_1^{(2)}\right|} e^{-(\sigma_1 - \sigma_2)t} \hat{\mathbf{u}}_2$$

Behavior of SALI for chaotic motion

The evolution of a deviation vector can be approximated by:

$$\mathbf{v}_1(t) = \sum_{i=1}^{n} c_i^{(1)} e^{\sigma_i t} \hat{u}_i \approx c_1^{(1)} e^{\sigma_1 t} \hat{u}_1 + c_2^{(1)} e^{\sigma_2 t} \hat{u}_2$$

where $\sigma_1 > \sigma_2 \geq \ldots \geq \sigma_n$ are the Lyapunov exponents. and $\hat{u}_j$ j=1, 2, …, 2N the corresponding eigendirections.

In this approximation, we derive a leading order estimate of the ratio

$$\frac{\mathbf{v}_1(t)}{\|\mathbf{v}_1(t)\|} \approx \frac{c_1^{(1)} e^{\sigma_1 t} \hat{u}_1 + c_2^{(1)} e^{\sigma_2 t} \hat{u}_2}{\left|c_1^{(1)}\right| e^{\sigma_1 t}} = \pm \hat{u}_1 + \frac{c_2^{(1)}}{\left|c_1^{(1)}\right|} e^{-(\sigma_1 - \sigma_2)t} \hat{u}_2$$

and an analogous expression for $\mathbf{v}_2$

$$\frac{\mathbf{v}_2(t)}{\|\mathbf{v}_2(t)\|} \approx \frac{c_1^{(2)} e^{\sigma_1 t} \hat{u}_1 + c_2^{(2)} e^{\sigma_2 t} \hat{u}_2}{\left|c_1^{(2)}\right| e^{\sigma_1 t}} = \pm \hat{u}_1 + \frac{c_2^{(2)}}{\left|c_1^{(2)}\right|} e^{-(\sigma_1 - \sigma_2)t} \hat{u}_2$$

So we get:

$$SALI(t) = \min\left\{ \left\| \frac{\mathbf{v}_1(t)}{\|\mathbf{v}_1(t)\|} + \frac{\mathbf{v}_2(t)}{\|\mathbf{v}_2(t)\|} \right\|, \left\| \frac{\mathbf{v}_1(t)}{\|\mathbf{v}_1(t)\|} - \frac{\mathbf{v}_2(t)}{\|\mathbf{v}_2(t)\|} \right\| \right\} \approx \left| \frac{c_2^{(1)}}{\left|c_1^{(1)}\right|} \pm \frac{c_2^{(2)}}{\left|c_1^{(2)}\right|} \right| e^{-(\sigma_1 - \sigma_2)t}$$

Behavior of SALI for chaotic motion

We test the validity of the approximation $SALI \propto e^{-(\sigma 1-\sigma 2)t}$ (Ch.S., Antonopoulos, Bountis, Vrahatis, 2004, J. Phys. A) for a chaotic orbit of the 3D Hamiltonian

$$H = \sum_{i=1}^{3} \frac{\omega_i}{2}(q_i^2 + p_i^2) + q_1^2 q_2 + q_1^2 q_3$$

with $\omega_1=1$, $\omega_2=1.4142$, $\omega_3=1.7321$, $H=0.09$

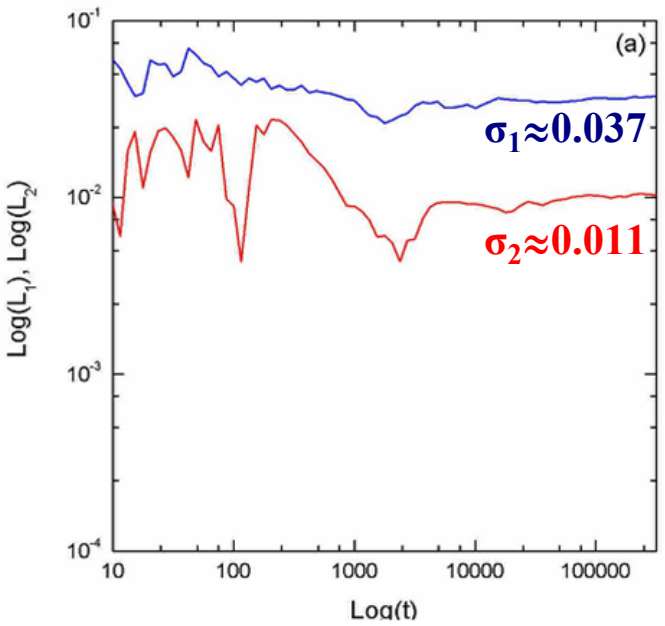

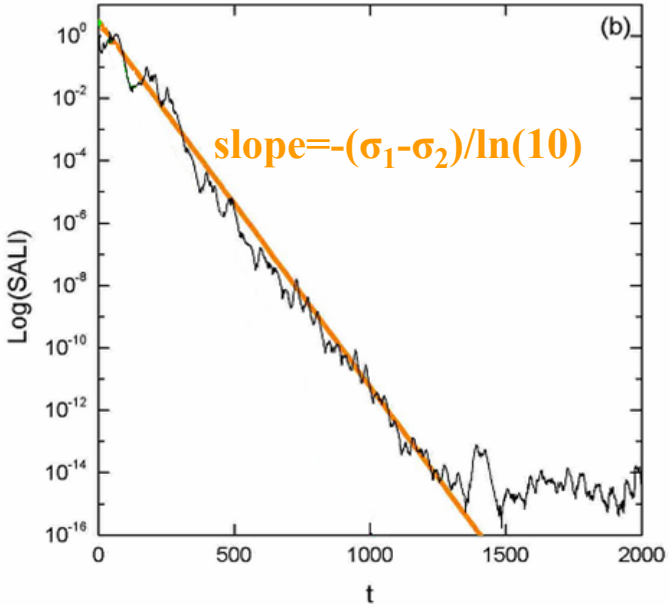

Behavior of SALI for regular motion

Regular motion occurs on a torus and two different initial deviation vectors become tangent to the torus, generally having different directions.

Behavior of SALI for regular motion

Regular motion occurs on a torus and two different initial deviation vectors become tangent to the torus, generally having different directions.

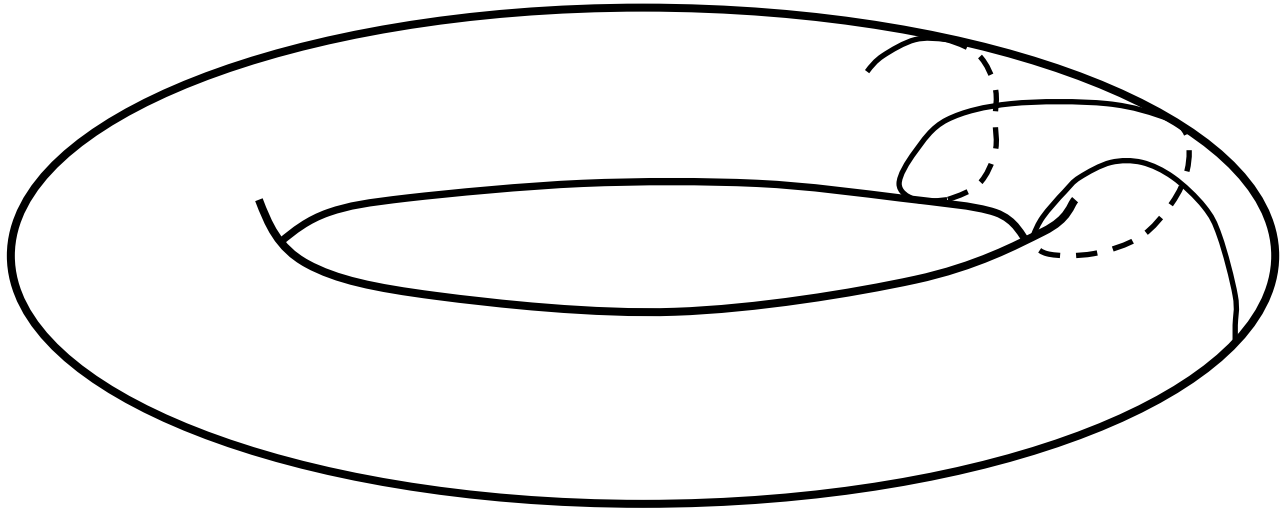

Behavior of SALI for regular motion

Regular motion occurs on a torus and two different initial deviation vectors become tangent to the torus, generally having different directions.

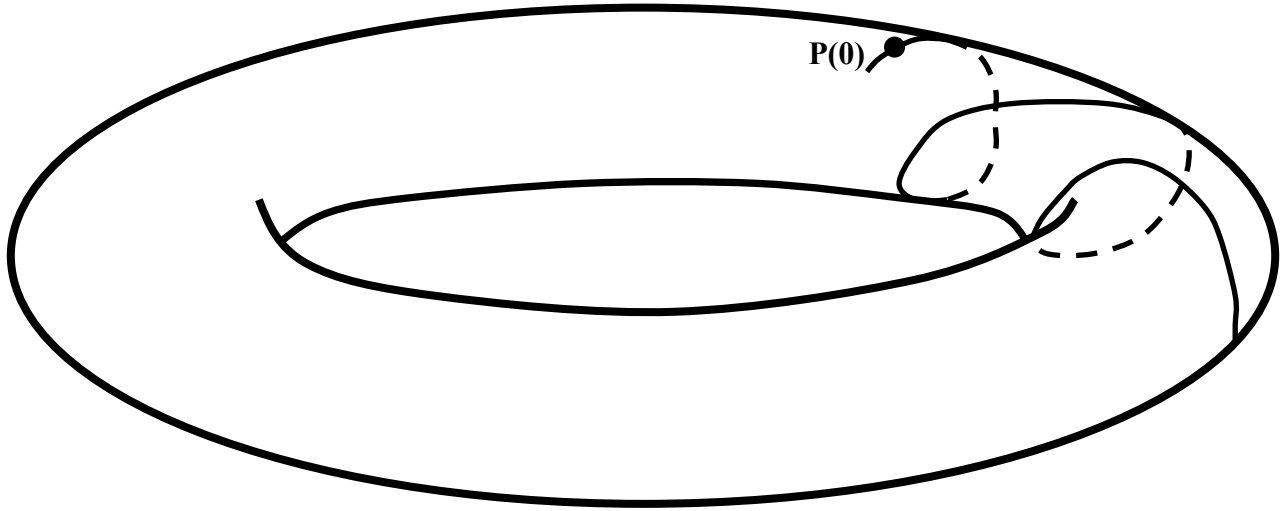

Behavior of SALI for regular motion

Regular motion occurs on a torus and two different initial deviation vectors become tangent to the torus, generally having different directions.

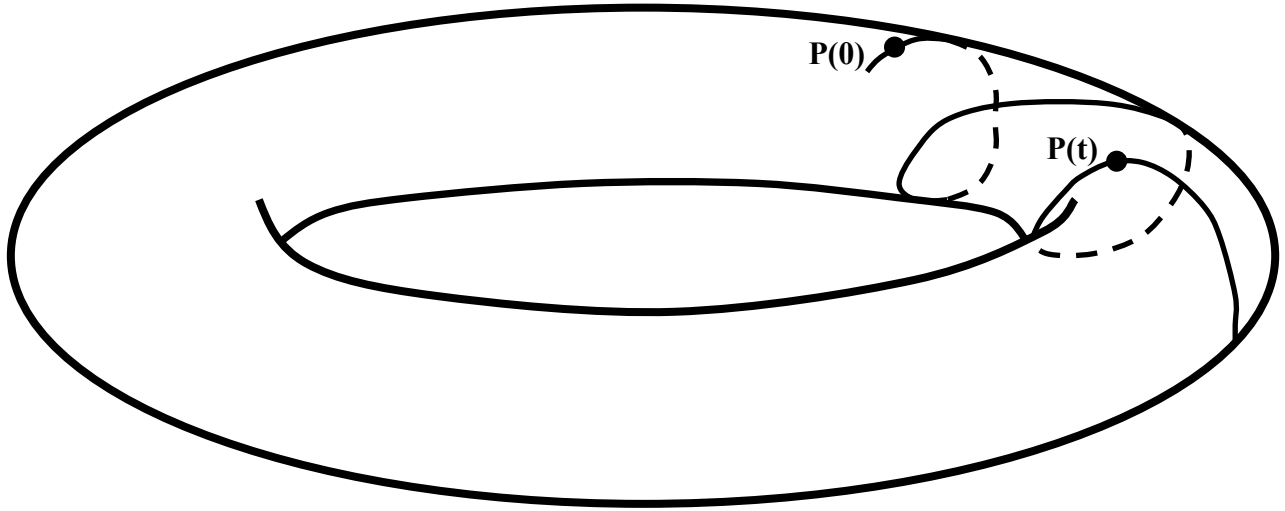

Behavior of SALI for regular motion

Regular motion occurs on a torus and two different initial deviation vectors become tangent to the torus, generally having different directions.

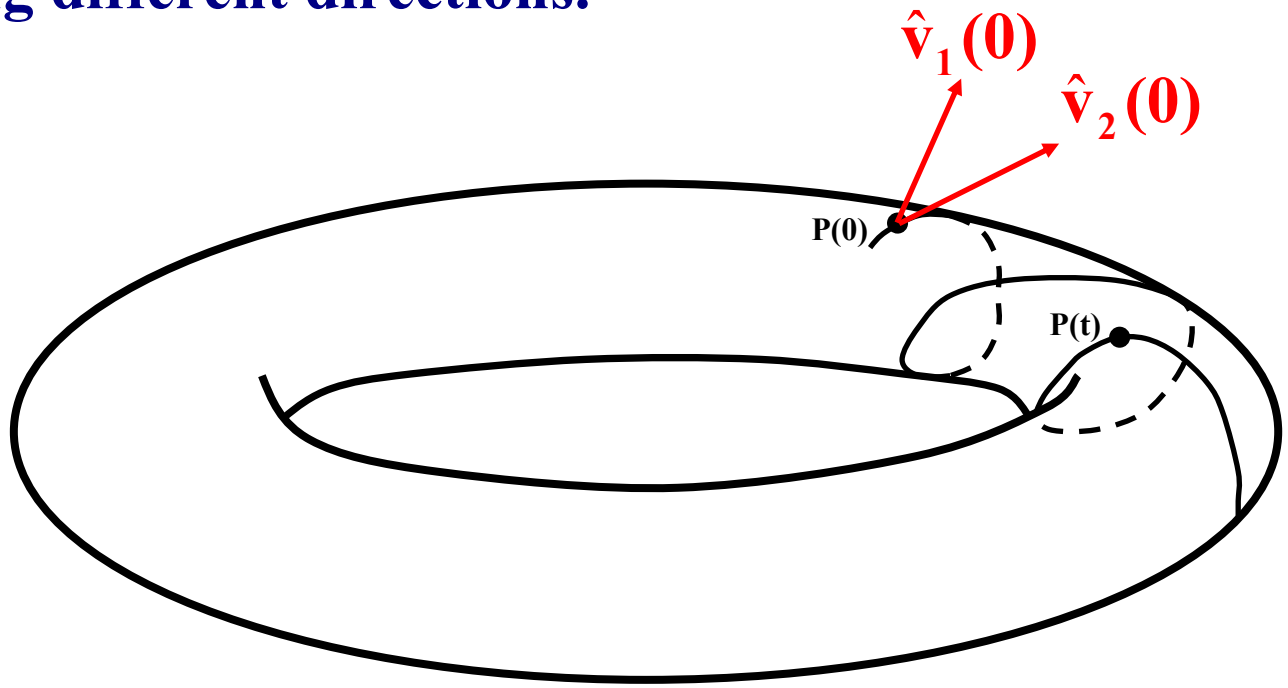

Behavior of SALI for regular motion

Regular motion occurs on a torus and two different initial deviation vectors become tangent to the torus, generally having different directions.

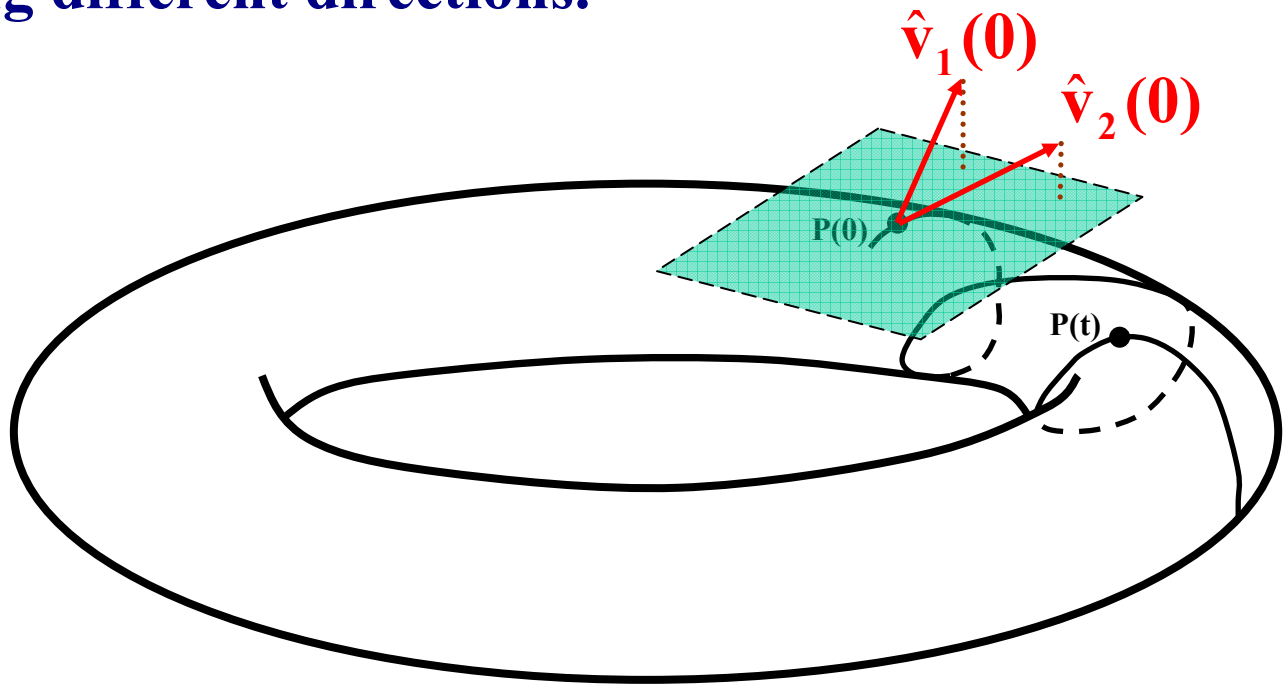

Behavior of SALI for regular motion

Regular motion occurs on a torus and two different initial deviation vectors become tangent to the torus, generally having different directions.

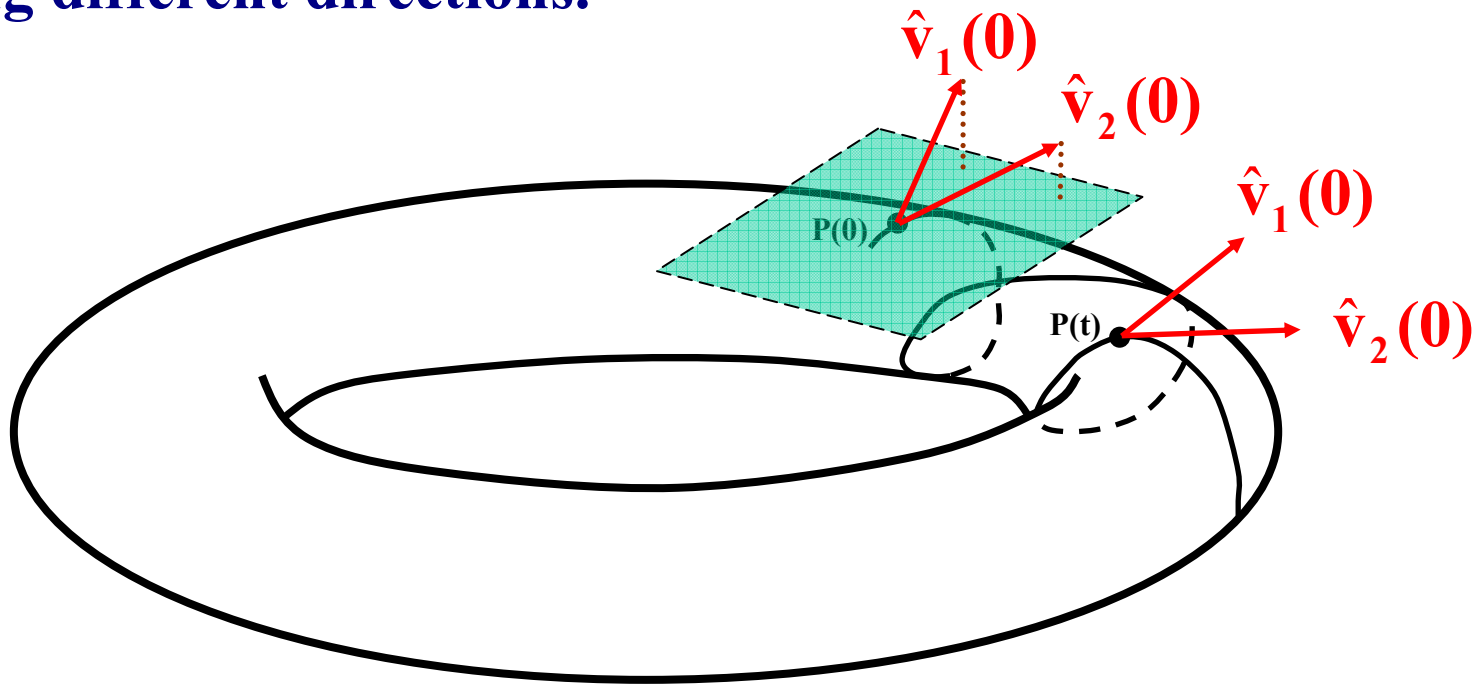

Behavior of SALI for regular motion

Regular motion occurs on a torus and two different initial deviation vectors become tangent to the torus, generally having different directions.

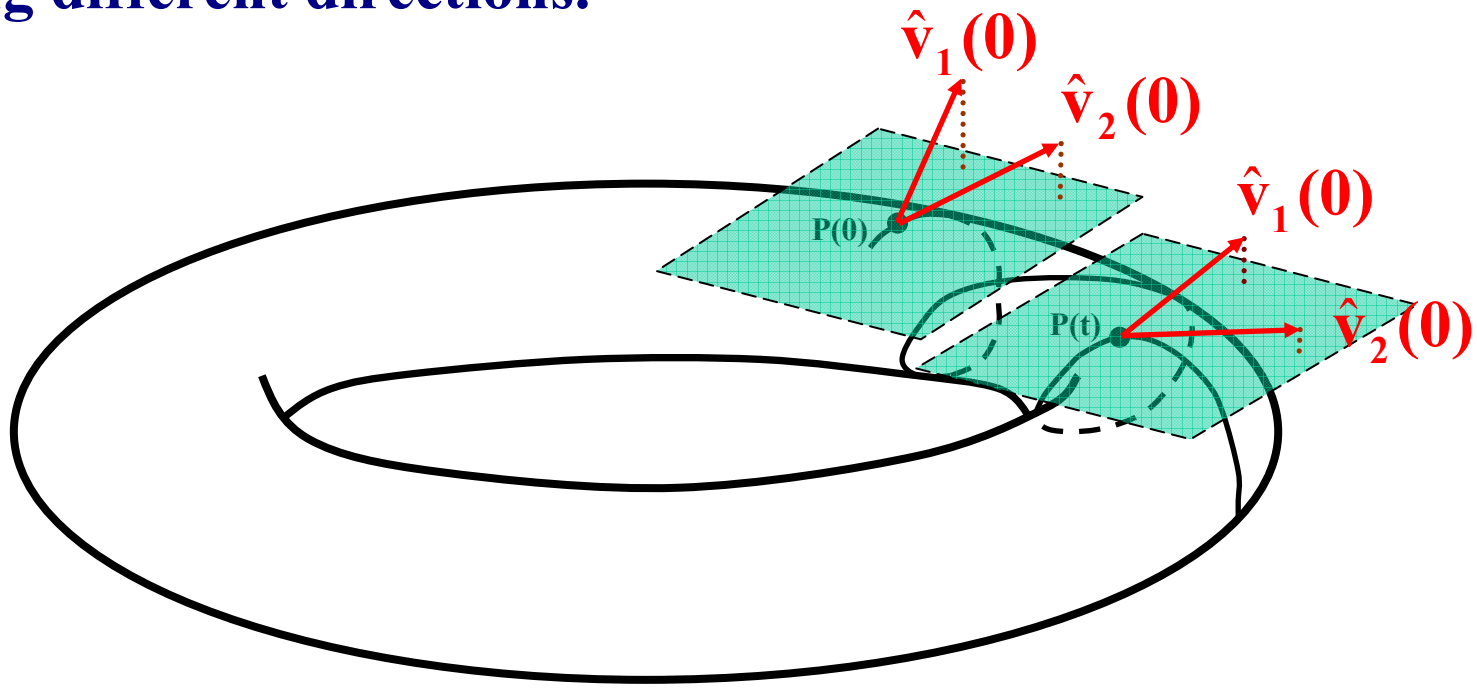

Applications – Hénon-Heiles system

As an example, we consider the 2D Hénon-Heiles system:

$$H_2 = \frac{1}{2}(p_x^2 + p_y^2) + \frac{1}{2}(x^2 + y^2) + x^2 y - \frac{1}{3}y^3$$

For E=1/8 we consider the orbits with initial conditions:
Regular orbit, x=0, y=0.55, p_x=0.2417, p_y=0
Chaotic orbit, x=0, y=-0.016, p_x=0.49974, p_y=0
Chaotic orbit, x=0, y=-0.01344, p_x=0.49982, p_y=0

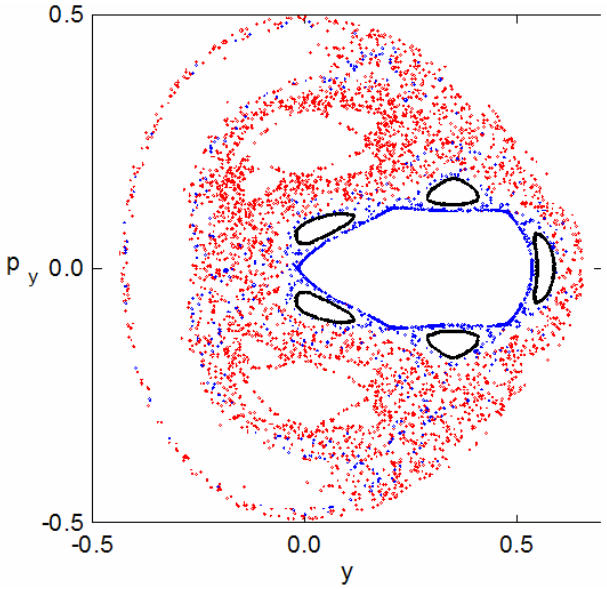

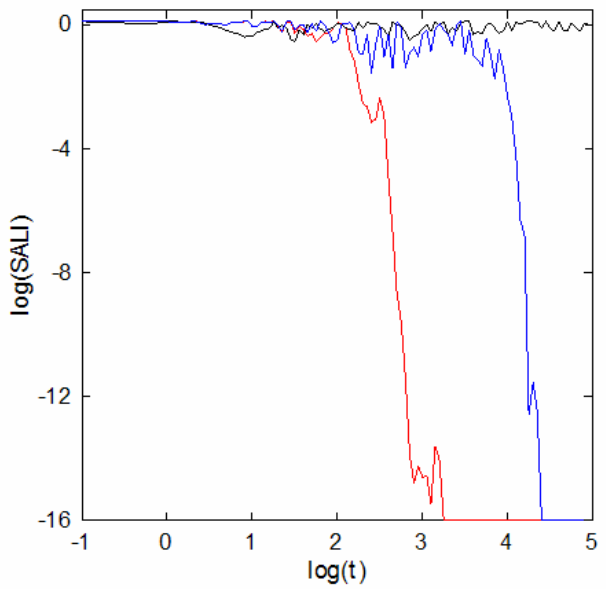

Applications – Hénon-Heiles system

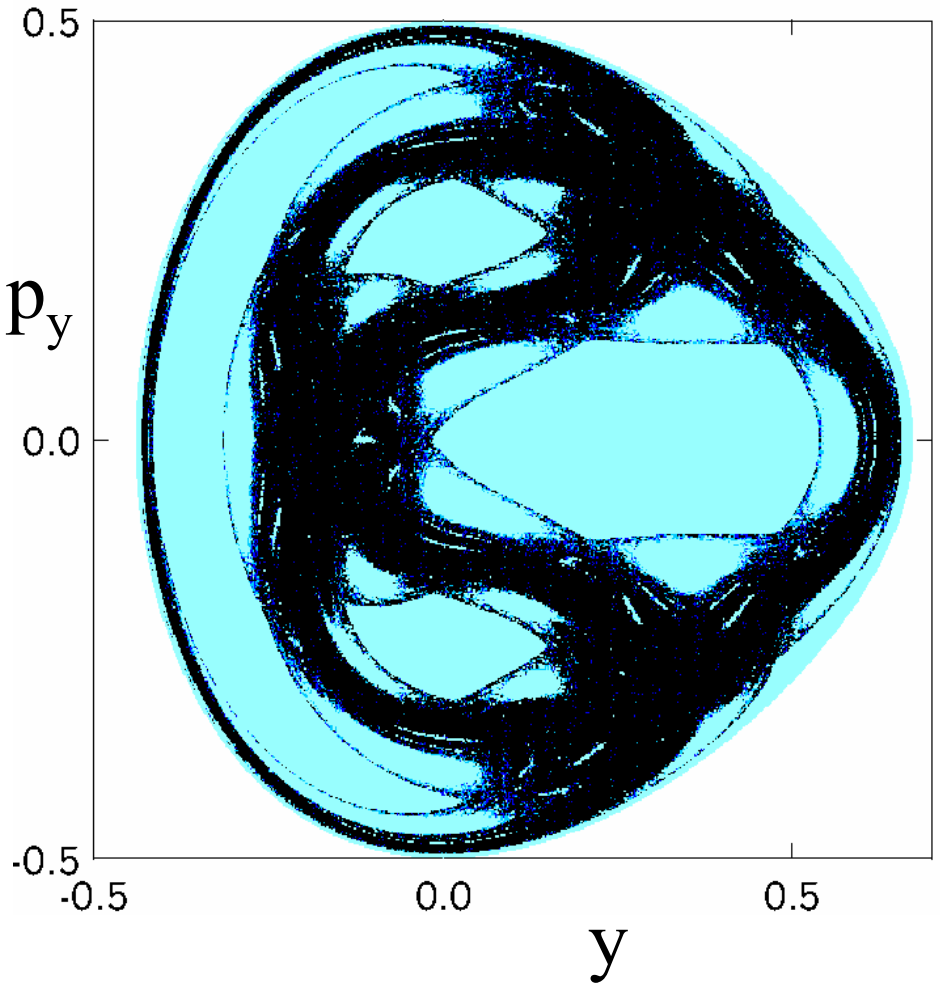

log(SALI) ≤ -12
-12 < log(SALI) ≤ -8
-8 < log(SALI) ≤ -4
-4 < log(SALI)

Applications – 4D map

$$
\begin{aligned}
x_1' &= x_1 + x_2 \\
x_2' &= x_2 - \nu \sin(x_1 + x_2) - \mu\,[1 - \cos(x_1 + x_2 + x_3 + x_4)] \\
x_3' &= x_3 + x_4 \\
x_4' &= x_4 - \kappa \sin(x_3 + x_4) - \mu\,[1 - \cos(x_1 + x_2 + x_3 + x_4)]
\end{aligned}
\qquad (\mathrm{mod}\ 2\pi)
$$

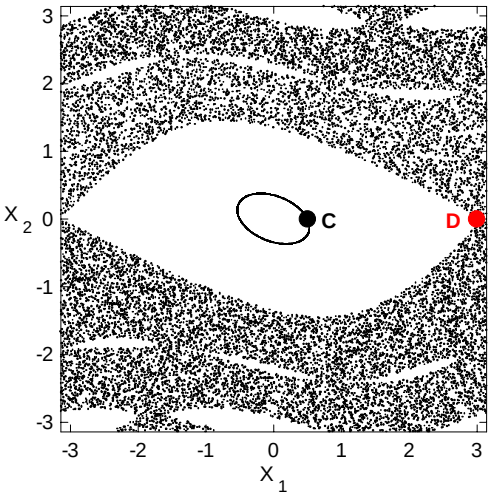

For ν=0.5, κ=0.1, μ=0.1 we consider the orbits:

regular orbit C *with initial conditions* $x_1=0.5$, $x_2=0$, $x_3=0.5$, $x_4=0$.

chaotic orbit D *with initial conditions* $x_1=3$, $x_2=0$, $x_3=0.5$, $x_4=0$.

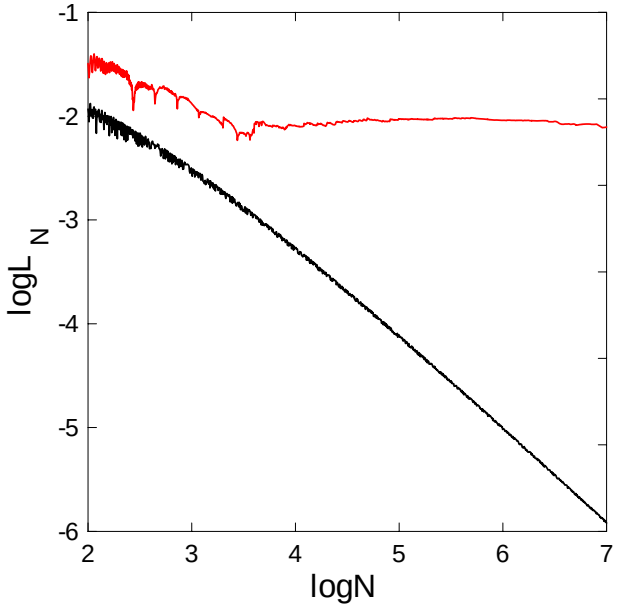

Applications – 4D map

$$
\begin{aligned}
x_1' &= x_1 + x_2 \\
x_2' &= x_2 - \nu \sin(x_1 + x_2) - \mu\,[1 - \cos(x_1 + x_2 + x_3 + x_4)] \\
x_3' &= x_3 + x_4 \\
x_4' &= x_4 - \kappa \sin(x_3 + x_4) - \mu\,[1 - \cos(x_1 + x_2 + x_3 + x_4)]
\end{aligned}
\qquad (\mathrm{mod}\ 2\pi)
$$

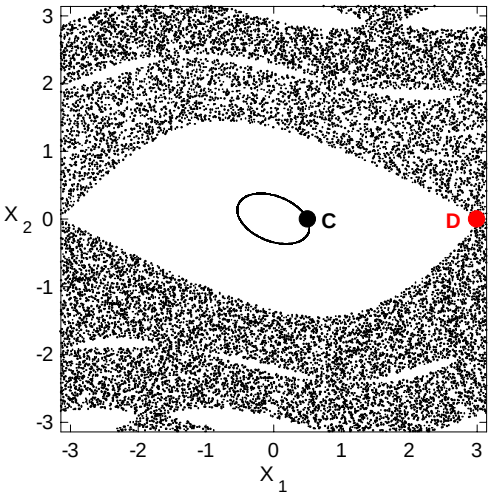

For ν=0.5, κ=0.1, μ=0.1 we consider the orbits:

regular orbit C *with initial conditions* $x_1=0.5$, $x_2=0$, $x_3=0.5$, $x_4=0$.

chaotic orbit D *with initial conditions* $x_1=3$, $x_2=0$, $x_3=0.5$, $x_4=0$.

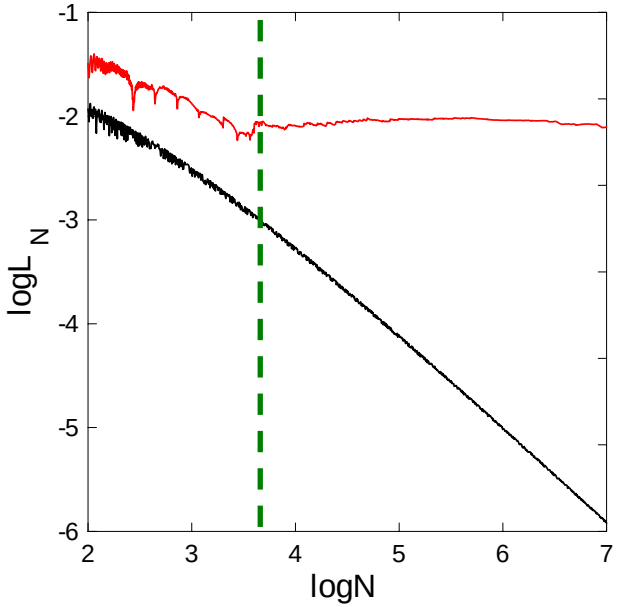

Applications – 4D map

$$
\begin{aligned}
x_1' &= x_1 + x_2 \\
x_2' &= x_2 - \nu \sin(x_1 + x_2) - \mu\,[1 - \cos(x_1 + x_2 + x_3 + x_4)] \\
x_3' &= x_3 + x_4 \\
x_4' &= x_4 - \kappa \sin(x_3 + x_4) - \mu\,[1 - \cos(x_1 + x_2 + x_3 + x_4)]
\end{aligned}
\qquad (\mathrm{mod}\ 2\pi)
$$

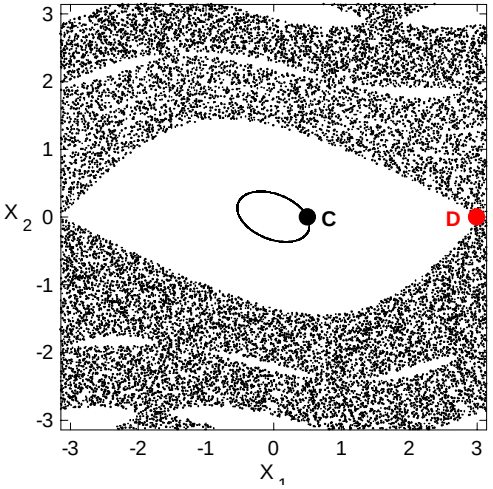

For ν=0.5, κ=0.1, μ=0.1 we consider the orbits:

regular orbit C *with initial conditions* $x_1=0.5$, $x_2=0$, $x_3=0.5$, $x_4=0$.

chaotic orbit D *with initial conditions* $x_1=3$, $x_2=0$, $x_3=0.5$, $x_4=0$.

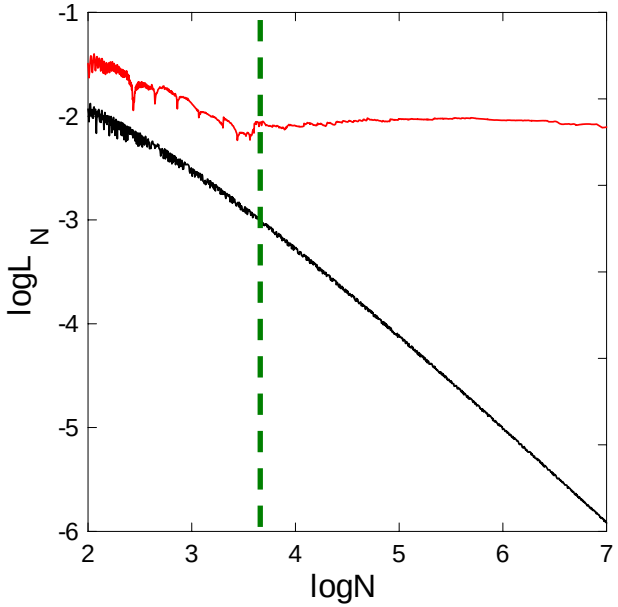

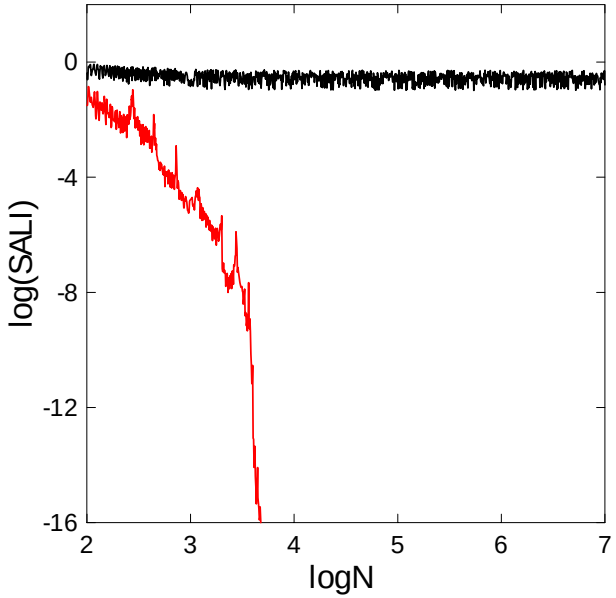

Applications – 4D map

$$
\begin{aligned}
x_1' &= x_1 + x_2 \\
x_2' &= x_2 - \nu \sin(x_1 + x_2) - \mu\,[1 - \cos(x_1 + x_2 + x_3 + x_4)] \\
x_3' &= x_3 + x_4 \\
x_4' &= x_4 - \kappa \sin(x_3 + x_4) - \mu\,[1 - \cos(x_1 + x_2 + x_3 + x_4)]
\end{aligned}
\qquad (\mathrm{mod}\ 2\pi)
$$

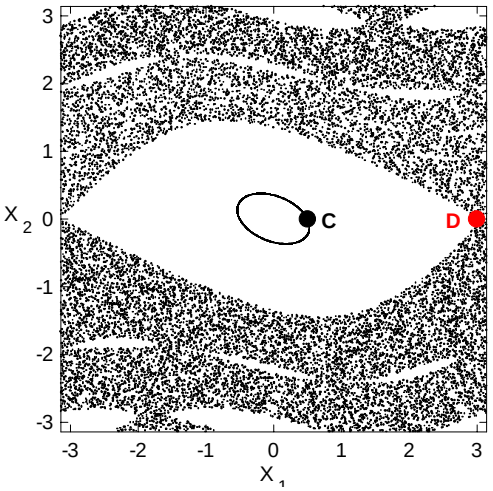

For ν=0.5, κ=0.1, μ=0.1 we consider the orbits:

regular orbit C *with initial conditions* $x_1=0.5$, $x_2=0$, $x_3=0.5$, $x_4=0$.

chaotic orbit D *with initial conditions* $x_1=3$, $x_2=0$, $x_3=0.5$, $x_4=0$.

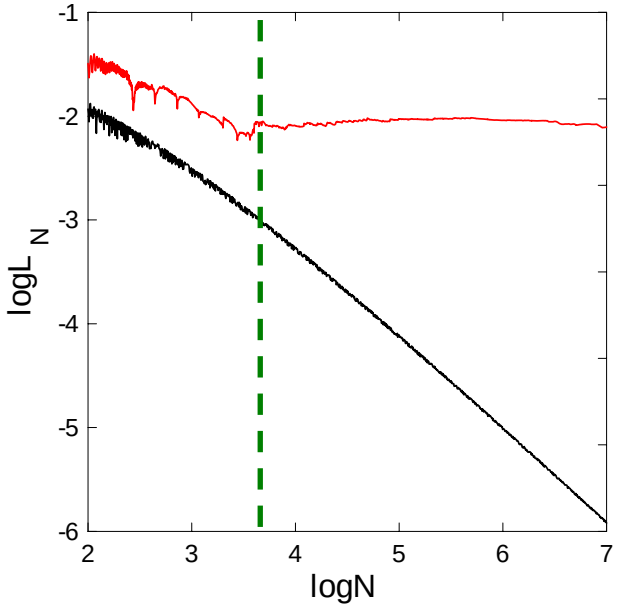

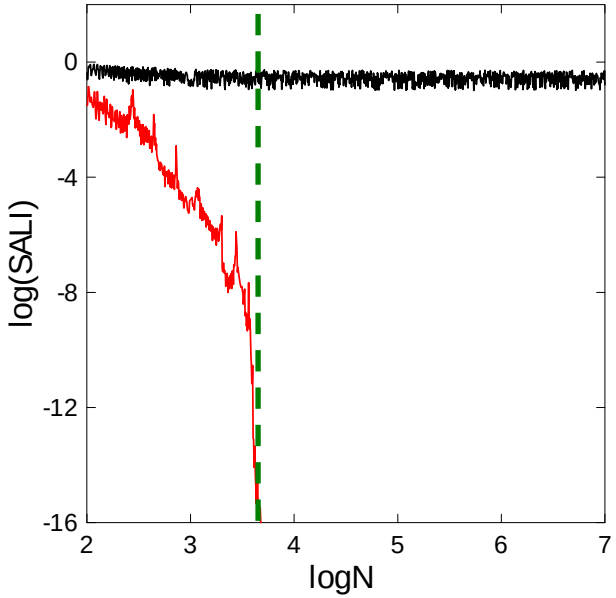

Applications – 4D Accelerator map

We consider the 4D symplectic map

$$\begin{pmatrix} x_1' \\ x_2' \\ x_3' \\ x_4' \end{pmatrix} = \begin{pmatrix} \cos\omega_1 & -\sin\omega_1 & 0 & 0 \\ \sin\omega_1 & \cos\omega_1 & 0 & 0 \\ 0 & 0 & \cos\omega_2 & -\sin\omega_2 \\ 0 & 0 & \sin\omega_2 & \cos\omega_2 \end{pmatrix} \times \begin{pmatrix} x_1 \\ x_2 + x_1^2 - x_3^2 \\ x_3 \\ x_4 - 2x_1x_3 \end{pmatrix}$$

describing the instantaneous sextupole 'kicks' experienced by a particle as it passes through an accelerator (Turchetti & Scandale 1991, Bountis & Tompaidis 1991, Vrahatis et al. 1996, 1997).

x_1 and x_3 are the particle's deflections from the ideal circular orbit, in the horizontal and vertical directions respectively.

x_2 and x_4 are the associated momenta

ω_1, ω_2 are related to the accelerator's tunes q_x, q_y by $\omega_1 = 2\pi q_x$, $\omega_2 = 2\pi q_y$

Our goal is to estimate the region of stability of the particle's motion, the so-called dynamic aperture of the beam (Bountis, Ch.S., 2006, Nucl. Inst Meth. Phys Res. A) and to increase its size using chaos control techniques (Boreaux, Carletti, Ch.S., Vittot, 2011, acc-ph/1007.1562 – Boreaux, Carletti, Ch.S., Papaphilippou, Vittot, 2011, Int. J. Bifur. Chaos, in press, acc-ph/1103.5631).

4D Accelerator map – "Global" study

Regions of different values of the SALI on the subspace $x_2(0)=x_4(0)=0$, after 10^5 iterations ($q_x=0.61803$ $q_y=0.4152$)

4D map

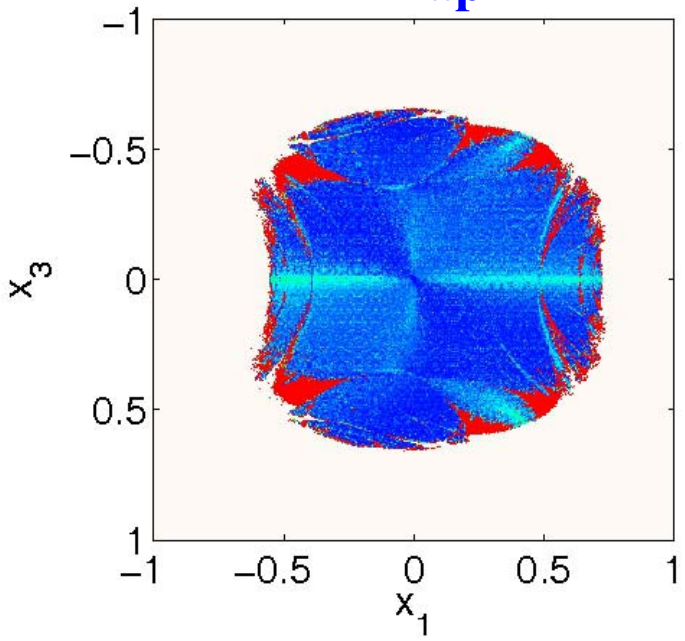

Controlled 4D map

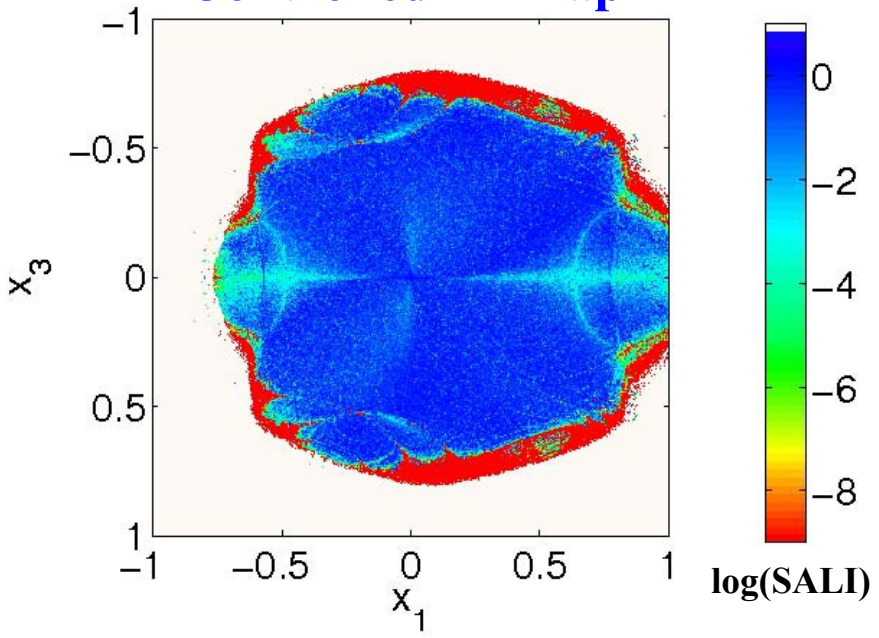

4D Accelerator map – "Global" study

Increase of the dynamic aperture

We evolve many orbits in 4D hyperspheres of radius r centered at $x_1=x_2=x_3=x_4=0$, for 10^5 iterations.

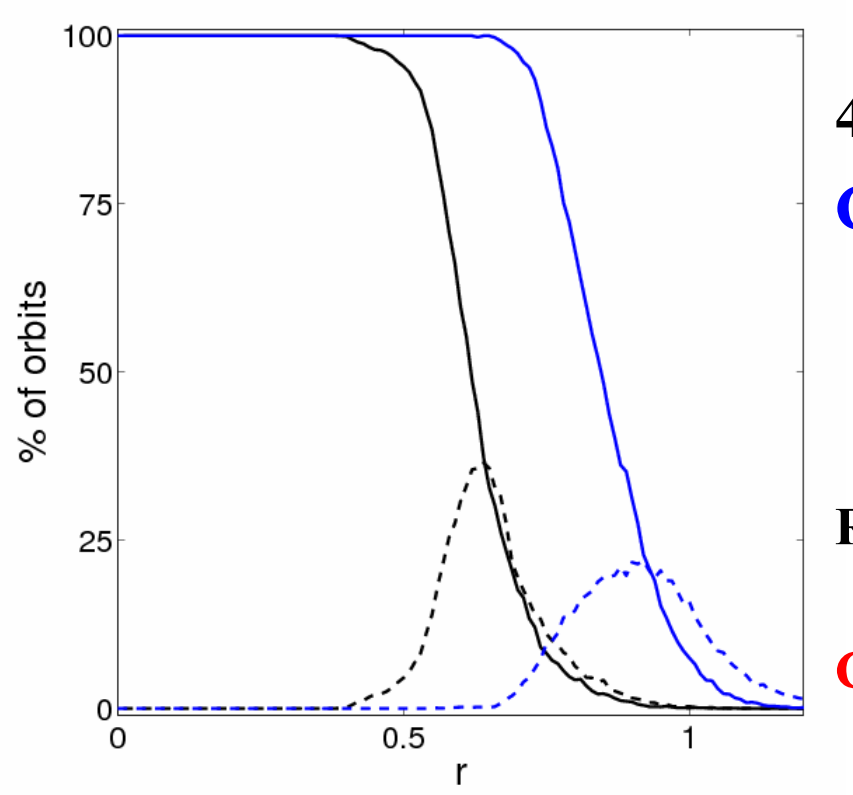

4D map

Controlled 4D map

Regular orbits

Chaotic orbits

Applications – 2D map

$$x_1' = x_1 + x_2$$
$$x_2' = x_2 - \nu \sin(x_1 + x_2) \quad \text{(mod } 2\pi\text{)}$$

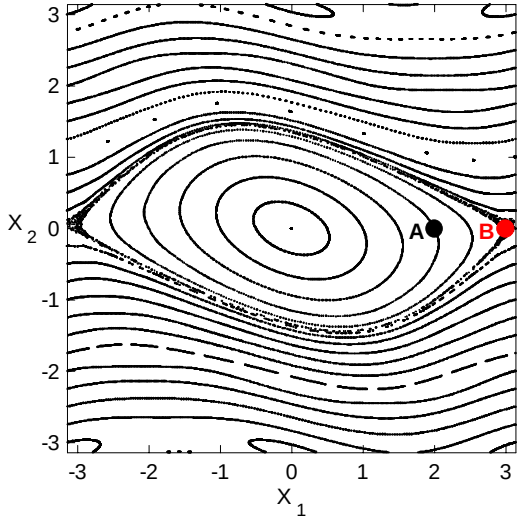

For ν=0.5 we consider the orbits:
regular orbit A *with initial conditions* $x_1=2$, $x_2=0$.
chaotic orbit B *with initial conditions* $x_1=3$, $x_2=0$.

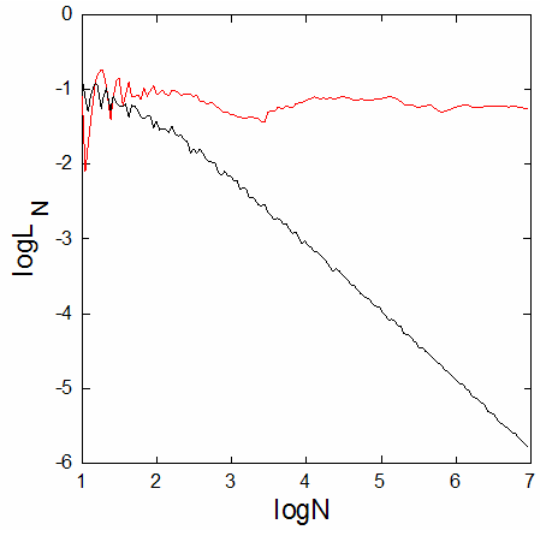

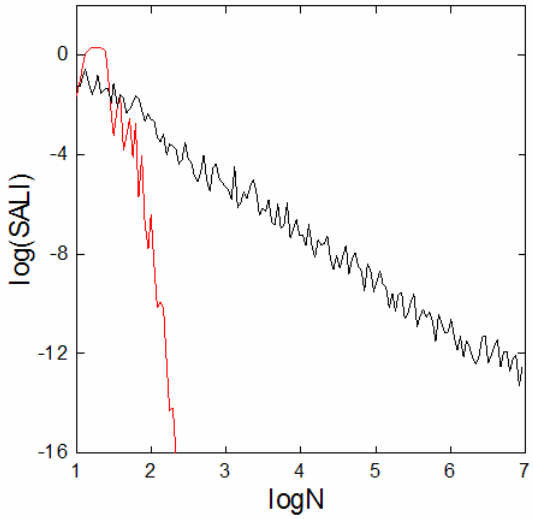

Behavior of SALI

2D maps

SALI→0 both for regular and chaotic orbits

following, however, completely different time rates which allows us to distinguish between the two cases.

Hamiltonian flows and multidimensional maps

SALI→0 for chaotic orbits

SALI→constant ≠ 0 for regular orbits

Questions

Can we generalize SALI so that the new index:

- **Can rapidly reveal the nature of chaotic orbits with $\sigma_1 \approx \sigma_2$ ($SALI \propto e^{-(\sigma 1 - \sigma 2)t}$)?**

- **Depends on several Lyapunov exponents for chaotic orbits?**

- **Exhibits power-law decay for regular orbits depending on the dimensionality of the tangent space of the reference orbit as for 2D maps?**

Definition of Generalized Alignment Index (GALI)

SALI effectively measures the 'area' of the parallelogram formed by the two deviation vectors.

Definition of Generalized Alignment Index (GALI)

SALI effectively measures the 'area' of the parallelogram formed by the two deviation vectors.

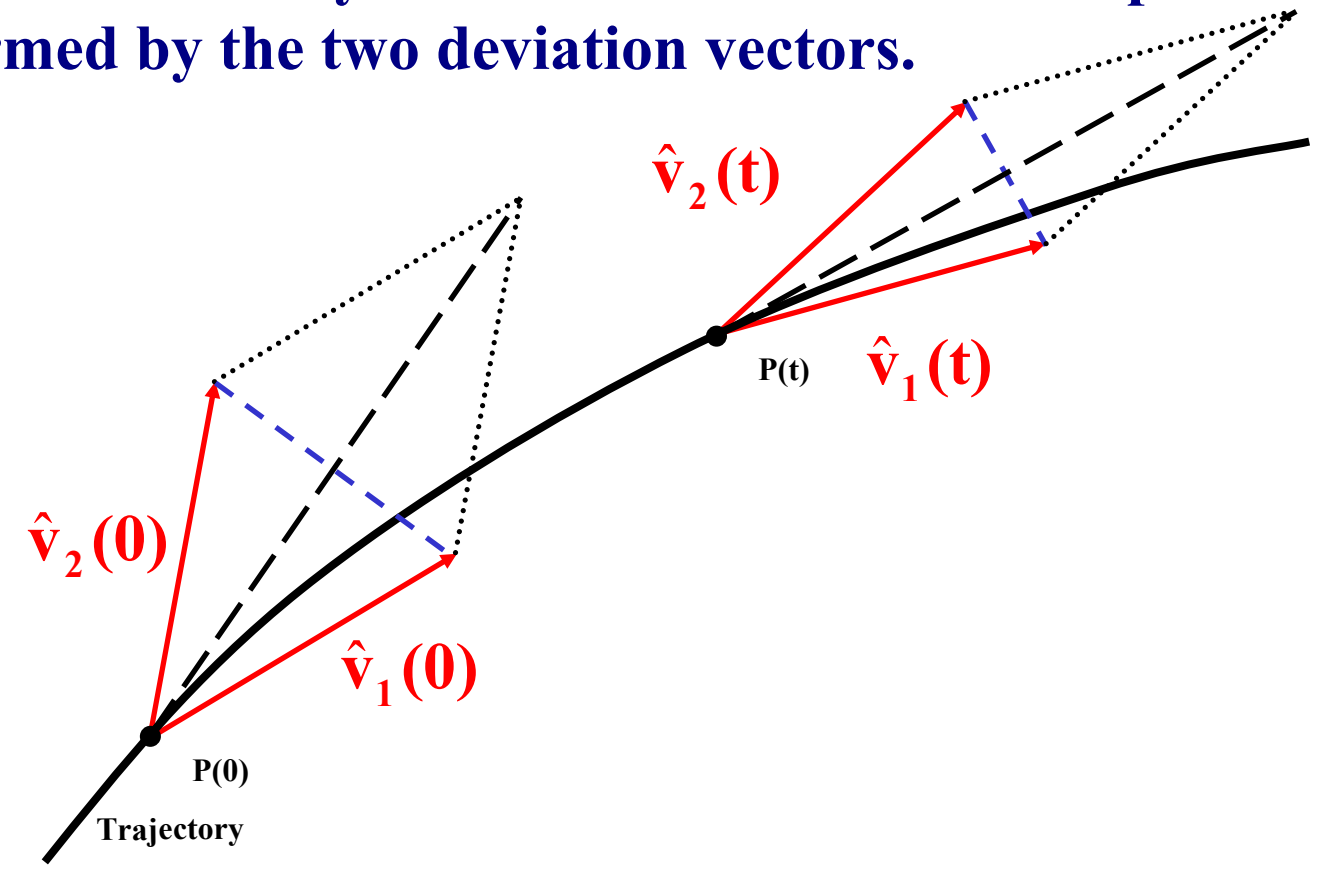

Definition of Generalized Alignment Index (GALI)

SALI effectively measures the 'area' of the parallelogram formed by the two deviation vectors.

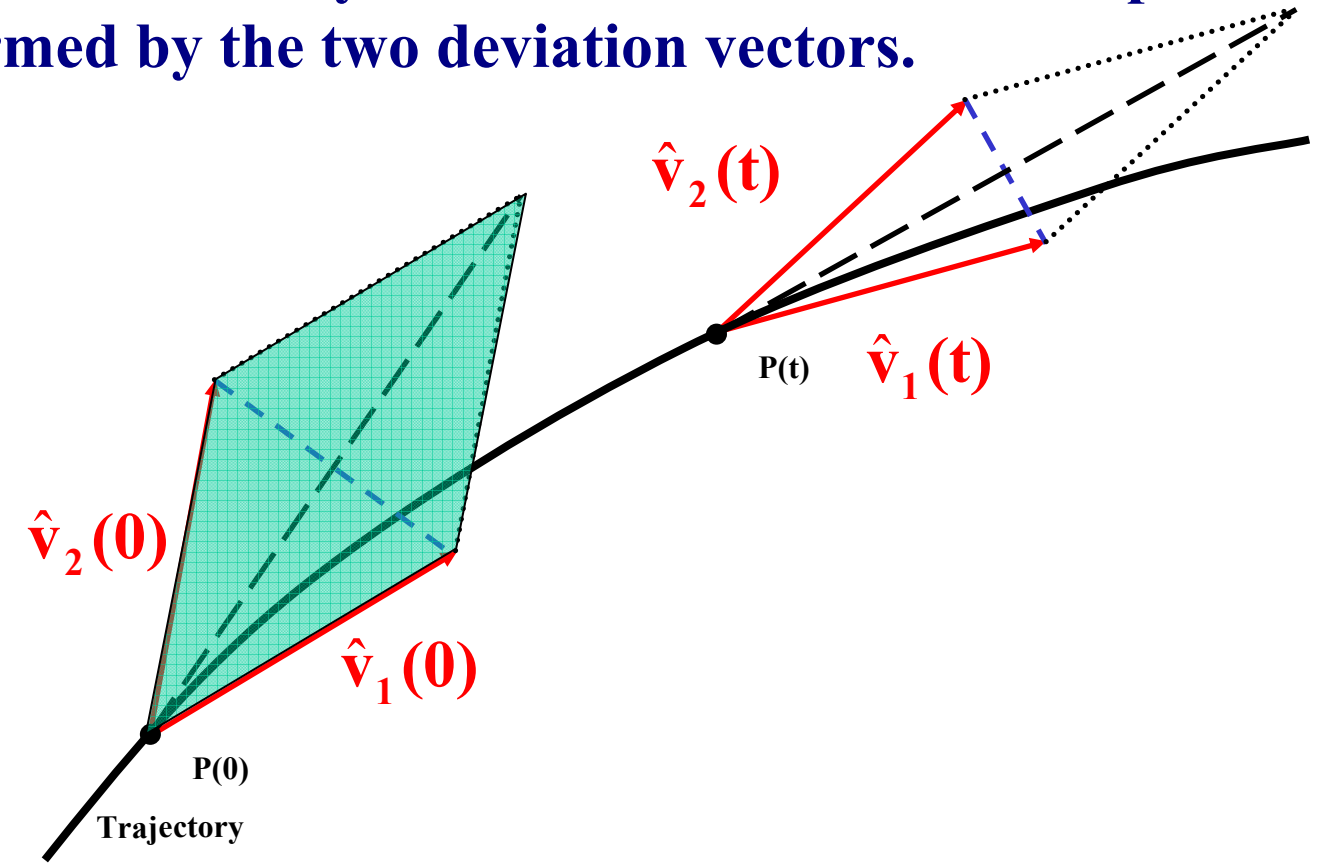

Definition of Generalized Alignment Index (GALI)

SALI effectively measures the 'area' of the parallelogram formed by the two deviation vectors.

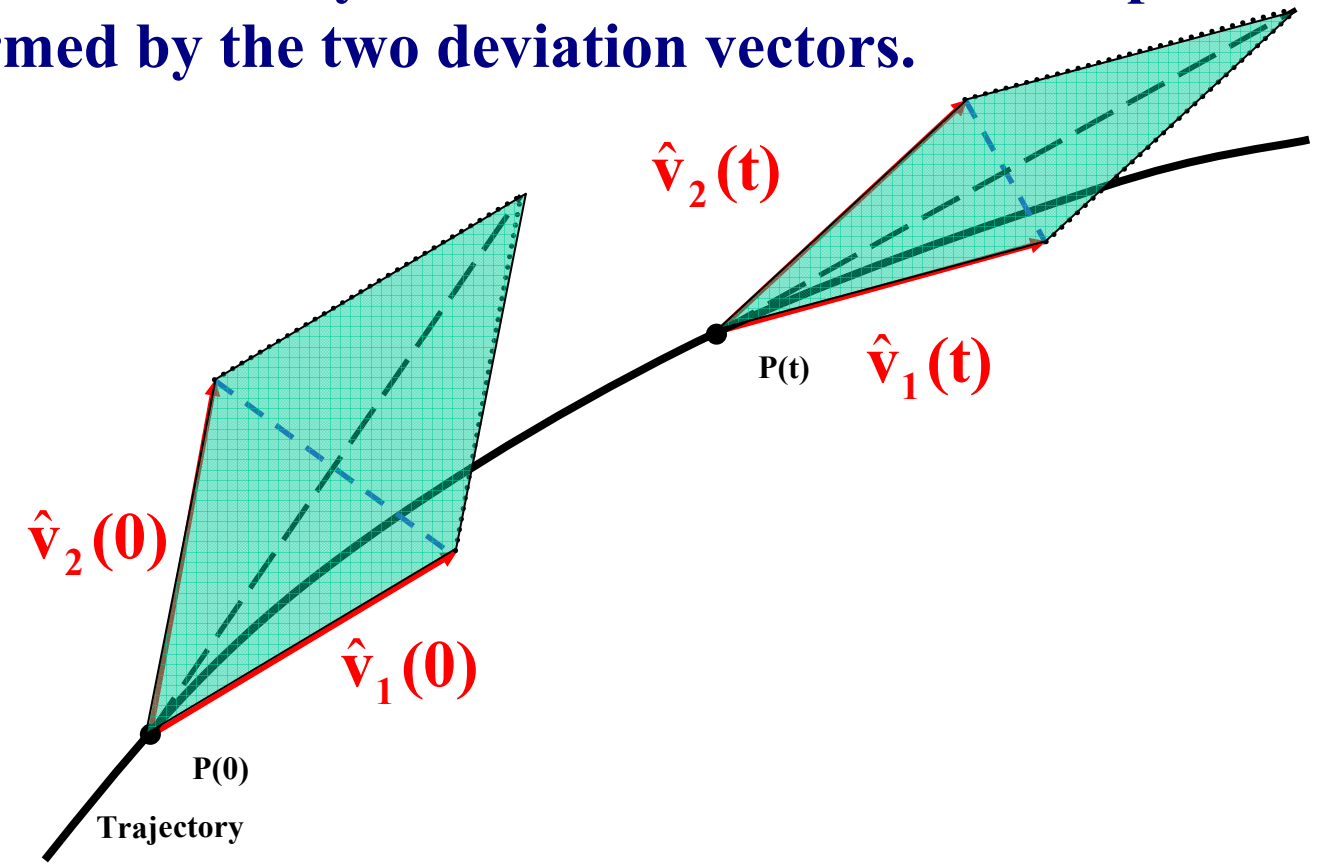

Definition of Generalized Alignment Index (GALI)

SALI effectively measures the 'area' of the parallelogram formed by the two deviation vectors.

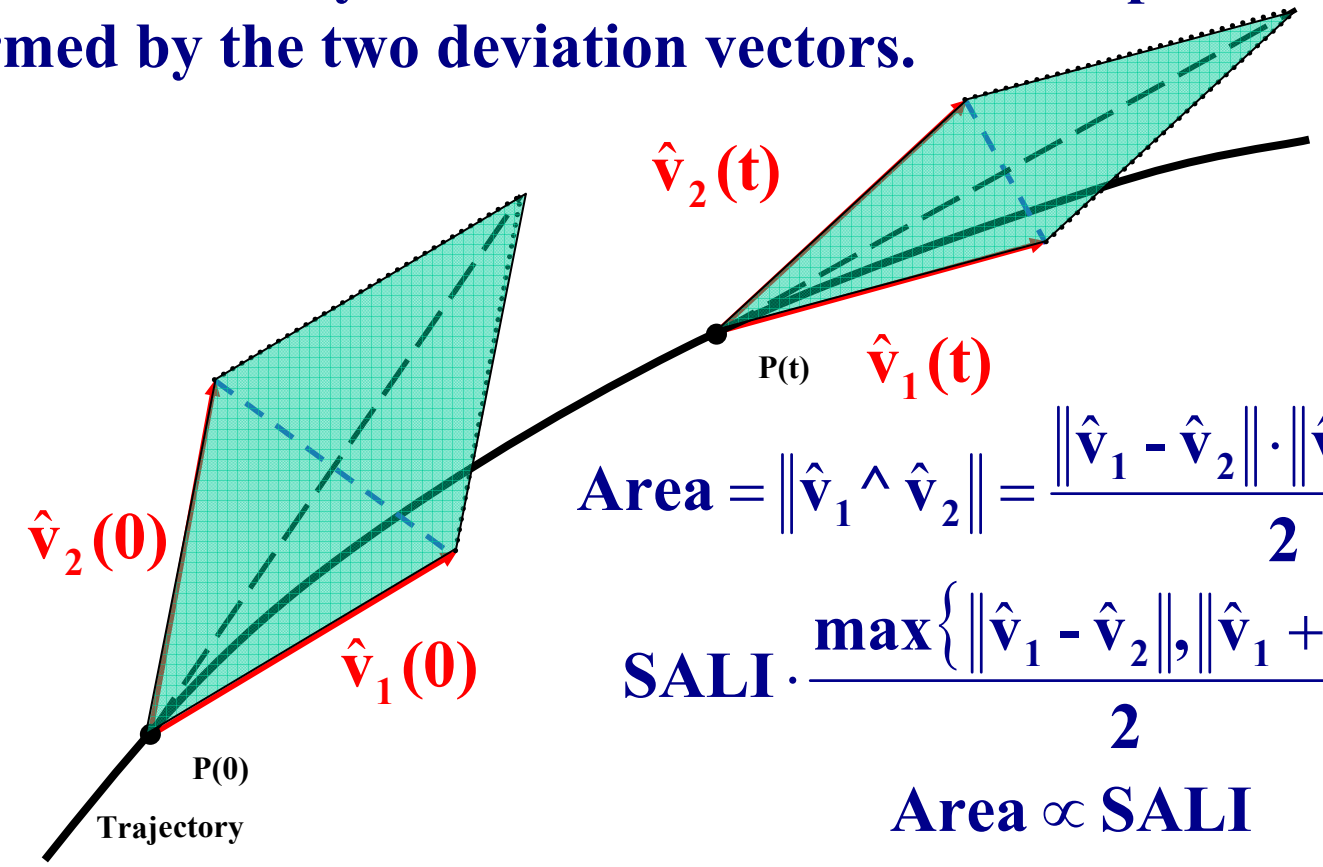

$$\text{Area} = \left\| \hat{v}_1 \wedge \hat{v}_2 \right\| = \frac{\left\| \hat{v}_1 - \hat{v}_2 \right\| \cdot \left\| \hat{v}_1 + \hat{v}_2 \right\|}{2} =$$

$$\text{SALI} \cdot \frac{\max\left\{ \left\| \hat{v}_1 - \hat{v}_2 \right\|, \left\| \hat{v}_1 + \hat{v}_2 \right\| \right\}}{2} \Rightarrow$$

$$\text{Area} \propto \text{SALI}$$

Definition of GALI

In the case of an N degree of freedom Hamiltonian system or a 2N symplectic map we follow the evolution of

k deviation vectors with $2 \leq k \leq 2N$,

and define (Ch.S., Bountis, Antonopoulos, 2007, Physica D) the Generalized Alignment Index (GALI) of order k :

$$GALI_k(t) = \left\| \hat{v}_1(t) \wedge \hat{v}_2(t) \wedge \ldots \wedge \hat{v}_k(t) \right\|$$

where

$$\hat{v}_1(t) = \frac{v_1(t)}{\left\| v_1(t) \right\|}$$

Wedge product

We consider as a basis of the 2N-dimensional tangent space of the system the usual set of orthonormal vectors:

$$\hat{e}_1 = (1,0,0,...,0),\ \hat{e}_2 = (0,1,0,...,0),\ ...,\ \hat{e}_{2N} = (0,0,0,...,1)$$

Then for k deviation vectors we have:

$$\begin{bmatrix} \hat{v}_1 \\ \hat{v}_2 \\ \vdots \\ \hat{v}_k \end{bmatrix} = \begin{bmatrix} v_{11} & v_{12} & \cdots & v_{1\,2N} \\ v_{21} & v_{22} & \cdots & v_{2\,2N} \\ \vdots & \vdots & & \vdots \\ v_{k1} & v_{k2} & \cdots & v_{k\,2N} \end{bmatrix} \cdot \begin{bmatrix} \hat{e}_1 \\ \hat{e}_2 \\ \vdots \\ \hat{e}_{2N} \end{bmatrix}$$

$$\hat{v}_1 \wedge \hat{v}_2 \wedge \cdots \wedge \hat{v}_k = \sum_{1 \le i_1 < i_2 < \cdots < i_k \le 2N} \begin{vmatrix} v_{1\,i_1} & v_{1\,i_2} & \cdots & v_{1\,i_k} \\ v_{2\,i_1} & v_{2\,i_2} & \cdots & v_{2\,i_k} \\ \vdots & \vdots & & \vdots \\ v_{k\,i_1} & v_{k\,i_2} & \cdots & v_{k\,i_k} \end{vmatrix} \hat{e}_{i_1} \wedge \hat{e}_{i_2} \wedge \cdots \wedge \hat{e}_{i_k}$$

Norm of wedge product

We define as 'norm' of the wedge product the quantity :

$$\left\| \hat{\mathbf{v}}_1 \wedge \hat{\mathbf{v}}_2 \wedge \cdots \wedge \hat{\mathbf{v}}_k \right\| = \left\{ \sum_{1 \le i_1 < i_2 < \cdots < i_k \le 2N} \begin{vmatrix} v_{1\,i_1} & v_{1\,i_2} & \cdots & v_{1\,i_k} \\ v_{2\,i_1} & v_{2\,i_2} & \cdots & v_{2\,i_k} \\ \vdots & \vdots & & \vdots \\ v_{k\,i_1} & v_{k\,i_2} & \cdots & v_{k\,i_k} \end{vmatrix}^2 \right\}^{1/2}$$

Computation of GALI - Example

Let us compute $GALI_3$ in the case of 2D Hamiltonian system (4-dimensional phase space).

$$\begin{bmatrix} \hat{v}_1 \\ \hat{v}_2 \\ \hat{v}_3 \end{bmatrix} = \begin{bmatrix} v_{11} & v_{12} & v_{13} & v_{14} \\ v_{21} & v_{22} & v_{23} & v_{24} \\ v_{31} & v_{32} & v_{33} & v_{34} \end{bmatrix} \cdot \begin{bmatrix} \hat{e}_1 \\ \hat{e}_2 \\ \hat{e}_3 \\ \hat{e}_4 \end{bmatrix}$$

Computation of GALI - Example

Let us compute $GALI_3$ in the case of 2D Hamiltonian system (4-dimensional phase space).

$$\begin{bmatrix} \hat{v}_1 \\ \hat{v}_2 \\ \hat{v}_3 \end{bmatrix} = \begin{bmatrix} v_{11} & v_{12} & v_{13} & v_{14} \\ v_{21} & v_{22} & v_{23} & v_{24} \\ v_{31} & v_{32} & v_{33} & v_{34} \end{bmatrix} \cdot \begin{bmatrix} \hat{e}_1 \\ \hat{e}_2 \\ \hat{e}_3 \\ \hat{e}_4 \end{bmatrix}$$

Columns 1 2 3

$$GALI_3 = \left\| \hat{v}_1 \wedge \hat{v}_2 \wedge \hat{v}_3 \right\| = \left\{ \begin{vmatrix} v_{11} & v_{12} & v_{13} \\ v_{21} & v_{22} & v_{23} \\ v_{31} & v_{32} & v_{33} \end{vmatrix}^2 + \right.$$

Computation of GALI - Example

Let us compute $GALI_3$ in the case of 2D Hamiltonian system (4-dimensional phase space).

$$\begin{bmatrix} \hat{v}_1 \\ \hat{v}_2 \\ \hat{v}_3 \end{bmatrix} = \begin{bmatrix} v_{11} & v_{12} & v_{13} & v_{14} \\ v_{21} & v_{22} & v_{23} & v_{24} \\ v_{31} & v_{32} & v_{33} & v_{34} \end{bmatrix} \cdot \begin{bmatrix} \hat{e}_1 \\ \hat{e}_2 \\ \hat{e}_3 \\ \hat{e}_4 \end{bmatrix}$$

$$GALI_3 = \left\| \hat{v}_1 \wedge \hat{v}_2 \wedge \hat{v}_3 \right\| = \left\{ \begin{vmatrix} v_{11} & v_{12} & v_{13} \\ v_{21} & v_{22} & v_{23} \\ v_{31} & v_{32} & v_{33} \end{vmatrix}^2 + \begin{vmatrix} v_{11} & v_{12} & v_{14} \\ v_{21} & v_{22} & v_{24} \\ v_{31} & v_{32} & v_{34} \end{vmatrix}^2 + \right.$$

Columns 1 2 3 1 2 4

Computation of GALI - Example

Let us compute $GALI_3$ in the case of 2D Hamiltonian system (4-dimensional phase space).

$$\begin{bmatrix} \hat{v}_1 \\ \hat{v}_2 \\ \hat{v}_3 \end{bmatrix} = \begin{bmatrix} v_{11} & v_{12} & v_{13} & v_{14} \\ v_{21} & v_{22} & v_{23} & v_{24} \\ v_{31} & v_{32} & v_{33} & v_{34} \end{bmatrix} \cdot \begin{bmatrix} \hat{e}_1 \\ \hat{e}_2 \\ \hat{e}_3 \\ \hat{e}_4 \end{bmatrix}$$

$$GALI_3 = \left\| \hat{v}_1 \wedge \hat{v}_2 \wedge \hat{v}_3 \right\| = \left\{ \begin{vmatrix} v_{11} & v_{12} & v_{13} \\ v_{21} & v_{22} & v_{23} \\ v_{31} & v_{32} & v_{33} \end{vmatrix}^2 + \begin{vmatrix} v_{11} & v_{12} & v_{14} \\ v_{21} & v_{22} & v_{24} \\ v_{31} & v_{32} & v_{34} \end{vmatrix}^2 + \right.$$

$$\left. \begin{vmatrix} v_{11} & v_{13} & v_{14} \\ v_{21} & v_{23} & v_{24} \\ v_{31} & v_{33} & v_{34} \end{vmatrix}^2 + \right.$$

Columns: 1 2 3 | 1 2 4 | 1 3 4

Computation of GALI - Example

Let us compute $GALI_3$ in the case of 2D Hamiltonian system (4-dimensional phase space).

$$\begin{bmatrix} \hat{v}_1 \\ \hat{v}_2 \\ \hat{v}_3 \end{bmatrix} = \begin{bmatrix} v_{11} & v_{12} & v_{13} & v_{14} \\ v_{21} & v_{22} & v_{23} & v_{24} \\ v_{31} & v_{32} & v_{33} & v_{34} \end{bmatrix} \cdot \begin{bmatrix} \hat{e}_1 \\ \hat{e}_2 \\ \hat{e}_3 \\ \hat{e}_4 \end{bmatrix}$$

$$GALI_3 = \left\| \hat{v}_1 \wedge \hat{v}_2 \wedge \hat{v}_3 \right\| = \left\{ \begin{vmatrix} v_{11} & v_{12} & v_{13} \\ v_{21} & v_{22} & v_{23} \\ v_{31} & v_{32} & v_{33} \end{vmatrix}^2 + \begin{vmatrix} v_{11} & v_{12} & v_{14} \\ v_{21} & v_{22} & v_{24} \\ v_{31} & v_{32} & v_{34} \end{vmatrix}^2 + \right.$$

$$\left. \begin{vmatrix} v_{11} & v_{13} & v_{14} \\ v_{21} & v_{23} & v_{24} \\ v_{31} & v_{33} & v_{34} \end{vmatrix}^2 + \begin{vmatrix} v_{12} & v_{13} & v_{14} \\ v_{22} & v_{23} & v_{24} \\ v_{32} & v_{33} & v_{34} \end{vmatrix}^2 \right\}^{1/2}$$

Columns: 1 2 3 | 1 2 4 | 1 3 4 | 2 3 4

Efficient computation of GALI

For k deviation vectors:

$$\begin{bmatrix} \hat{v}_1 \\ \hat{v}_2 \\ \vdots \\ \hat{v}_k \end{bmatrix} = \begin{bmatrix} v_{11} & v_{12} & \cdots & v_{1\,2N} \\ v_{21} & v_{22} & \cdots & v_{2\,2N} \\ \vdots & \vdots & & \vdots \\ v_{k1} & v_{k2} & \cdots & v_{k\,2N} \end{bmatrix} \cdot \begin{bmatrix} \hat{e}_1 \\ \hat{e}_2 \\ \vdots \\ \hat{e}_{2N} \end{bmatrix} = A \cdot \begin{bmatrix} \hat{e}_1 \\ \hat{e}_2 \\ \vdots \\ \hat{e}_{2N} \end{bmatrix}$$

the 'norm' of the wedge product is given by:

$$\left\| \hat{v}_1 \wedge \hat{v}_2 \wedge \cdots \wedge \hat{v}_k \right\| = \left\{ \sum_{1 \le i_1 < i_2 < \cdots < i_k \le 2N} \begin{vmatrix} v_{1\,i_1} & v_{1\,i_2} & \cdots & v_{1\,i_k} \\ v_{2\,i_1} & v_{2\,i_2} & \cdots & v_{2\,i_k} \\ \vdots & \vdots & & \vdots \\ v_{k\,i_1} & v_{k\,i_2} & \cdots & v_{k\,i_k} \end{vmatrix}^2 \right\}^{1/2} = \sqrt{\det(A \cdot A^T)}$$

Efficient computation of GALI

From Singular Value Decomposition (SVD) of A^T we get:

$$A^T = U \cdot W \cdot V^T$$

where U is a column-orthogonal 2N×k matrix ($U^T \cdot U = I$), V^T is a k×k orthogonal matrix ($V \cdot V^T = I$), and W is a diagonal k×k matrix with positive or zero elements, the so-called singular values. So, we get:

$$\det(A \cdot A^T) = \det(V \cdot W^T \cdot U^T \cdot U \cdot W \cdot V^T) = \det(V \cdot W \cdot I \cdot W \cdot V^T) =$$

$$\det(V \cdot W^2 \cdot V^T) = \det(V \cdot \mathrm{diag}(w_1^2, w_2^2, \ldots w_k^2) \cdot V^T) = \prod_{i=1}^{k} w_i^2$$

Thus, $GALI_k$ is computed by:

$$GALI_k = \sqrt{\det(A \cdot A^T)} = \prod_{i=1}^{k} w_i \Rightarrow \log(GALI_k) = \sum_{i=1}^{k} \log(w_i)$$

Behavior of $GALI_k$ for chaotic motion

$GALI_k$ $(2 \leq k \leq 2N)$ tends exponentially to zero with exponents that involve the values of the first k largest Lyapunov exponents $\sigma_1, \sigma_2, \ldots, \sigma_k$:

$$GALI_k(t) \propto e^{-[(\sigma_1-\sigma_2)+(\sigma_1-\sigma_3)+\ldots+(\sigma_1-\sigma_k)]t}$$

The above relation is valid even if some Lyapunov exponents are equal, or very close to each other.

Behavior of $GALI_k$ for chaotic motion

Using the approximation:

$$\mathbf{v}_i(t) = \sum_{j=1}^{2N} c_j^i e^{\sigma_j t}\hat{u}_j = c_1^i e^{\sigma_1 t}\hat{u}_1 + c_2^i e^{\sigma_2 t}\hat{u}_2 + \cdots + c_{2N}^i e^{\sigma_{2N} t}\hat{u}_{2N}, \qquad \|\mathbf{v}_i(t)\| \approx \left|c_1^i\right| e^{\sigma_1 t}$$

where $\sigma_1 > \sigma_2 \geq \ldots \geq \sigma_n$ are the Lyapunov exponents, and $\hat{u}_j$ j=1, 2, …, 2N the corresponding eigendirections, we get

$$\begin{bmatrix} \hat{v}_1 \\ \hat{v}_2 \\ \vdots \\ \hat{v}_k \end{bmatrix} = \begin{bmatrix} s_1 & \frac{c_2^1}{|c_1^1|} e^{-(\sigma_1-\sigma_2)t} & \frac{c_3^1}{|c_1^1|} e^{-(\sigma_1-\sigma_3)t} & \cdots & \frac{c_{2N}^1}{|c_1^1|} e^{-(\sigma_1-\sigma_{2N})t} \\ s_2 & \frac{c_2^2}{|c_1^2|} e^{-(\sigma_1-\sigma_2)t} & \frac{c_3^2}{|c_1^2|} e^{-(\sigma_1-\sigma_3)t} & \cdots & \frac{c_{2N}^2}{|c_1^2|} e^{-(\sigma_1-\sigma_{2N})t} \\ \vdots & \vdots & \vdots & & \vdots \\ s_k & \frac{c_2^k}{|c_1^k|} e^{-(\sigma_1-\sigma_2)t} & \frac{c_3^k}{|c_1^k|} e^{-(\sigma_1-\sigma_3)t} & \cdots & \frac{c_{2N}^k}{|c_1^k|} e^{-(\sigma_1-\sigma_{2N})t} \end{bmatrix} \cdot \begin{bmatrix} \hat{u}_1 \\ \hat{u}_2 \\ \vdots \\ \hat{u}_{2N} \end{bmatrix}$$

with $s_i = \text{sign}(c_1^i)$.

Behavior of $GALI_k$ for chaotic motion

From all determinants appearing in the definition of $GALI_k$ the one that decreases the slowest is the one containing the first k columns of the previous matrix:

$$\begin{vmatrix} s_1 & \frac{c_2^1}{|c_1^1|}e^{-(\sigma_1-\sigma_2)t} & \frac{c_3^1}{|c_1^1|}e^{-(\sigma_1-\sigma_3)t} & \cdots & \frac{c_k^1}{|c_1^1|}e^{-(\sigma_1-\sigma_k)t} \\ s_2 & \frac{c_2^2}{|c_1^2|}e^{-(\sigma_1-\sigma_2)t} & \frac{c_3^2}{|c_1^2|}e^{-(\sigma_1-\sigma_3)t} & \cdots & \frac{c_k^2}{|c_1^2|}e^{-(\sigma_1-\sigma_k)t} \\ \vdots & \vdots & \vdots & & \vdots \\ s_k & \frac{c_2^k}{|c_1^k|}e^{-(\sigma_1-\sigma_2)t} & \frac{c_3^k}{|c_1^k|}e^{-(\sigma_1-\sigma_3)t} & \cdots & \frac{c_k^k}{|c_1^k|}e^{-(\sigma_1-\sigma_k)t} \end{vmatrix} = \begin{vmatrix} s_1 & \frac{c_2^1}{|c_1^1|} & \frac{c_3^1}{|c_1^1|} & \cdots & \frac{c_k^1}{|c_1^1|} \\ s_2 & \frac{c_2^2}{|c_1^2|} & \frac{c_3^2}{|c_1^2|} & \cdots & \frac{c_k^2}{|c_1^2|} \\ \vdots & \vdots & \vdots & & \vdots \\ s_k & \frac{c_2^k}{|c_1^k|} & \frac{c_3^k}{|c_1^k|} & \cdots & \frac{c_k^k}{|c_1^k|} \end{vmatrix} \cdot e^{-[(\sigma_1-\sigma_2)+(\sigma_1-\sigma_3)+\cdots+(\sigma_1-\sigma_k)]t}$$

Thus

$$GALI_k(t) \propto e^{-[(\sigma_1-\sigma_2)+(\sigma_1-\sigma_3)+\ldots+(\sigma_1-\sigma_k)]t}$$

Behavior of $GALI_k$ for chaotic motion

2D Hamiltonian (Hénon-Heiles system)

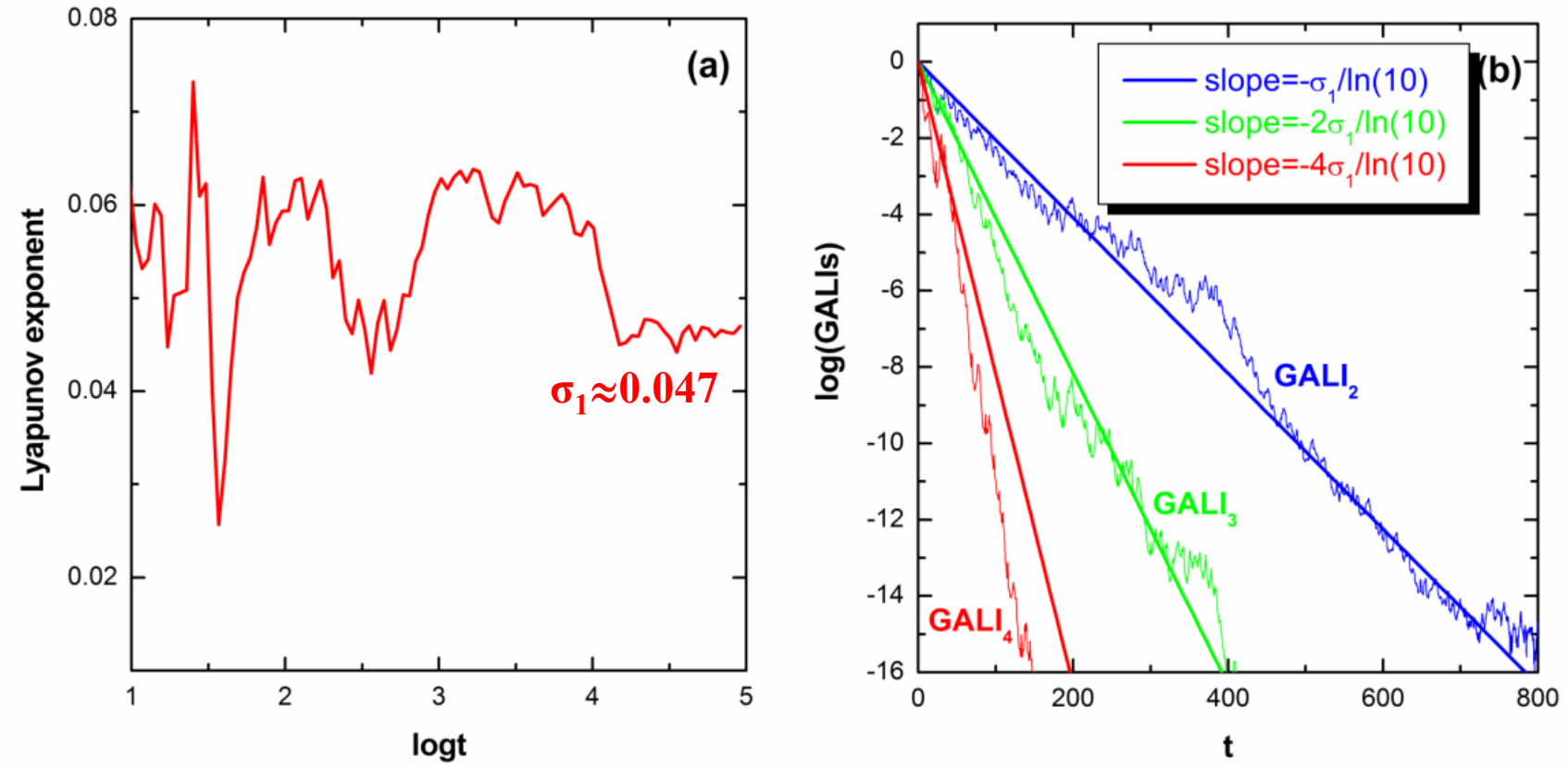

Behavior of $GALI_k$ for chaotic motion

3D system:

$$H_3 = \sum_{i=1}^{3} \frac{\omega_i}{2}(q_i^2 + p_i^2) + q_1^2 q_2 + q_1^2 q_3$$

with $\omega_1=1$, $\omega_2=\sqrt{2}$, $\omega_3=\sqrt{3}$, $H_3=0.09$.

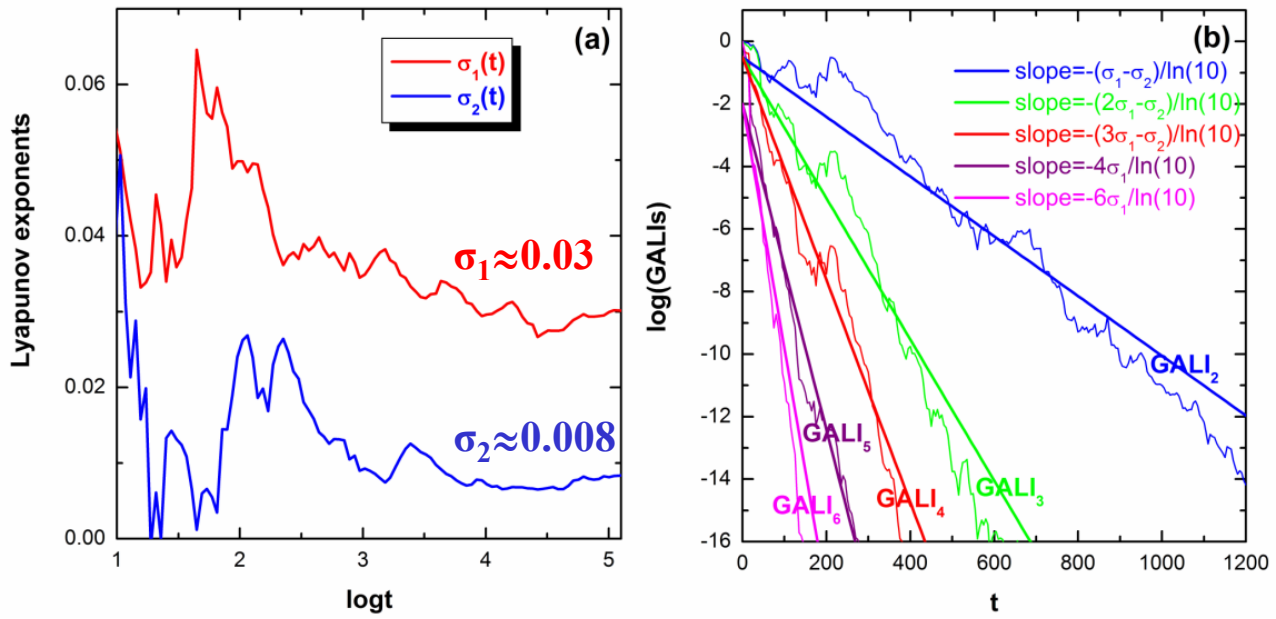

Behavior of $GALI_k$ for chaotic motion

N particles Fermi-Pasta-Ulam (FPU) system:

$$H = \frac{1}{2}\sum_{i=1}^{N} p_i^2 + \sum_{i=0}^{N}\left[\frac{1}{2}(q_{i+1} - q_i)^2 + \frac{\beta}{4}(q_{i+1} - q_i)^4\right]$$

with fixed boundary conditions, N=8 and β=1.5.

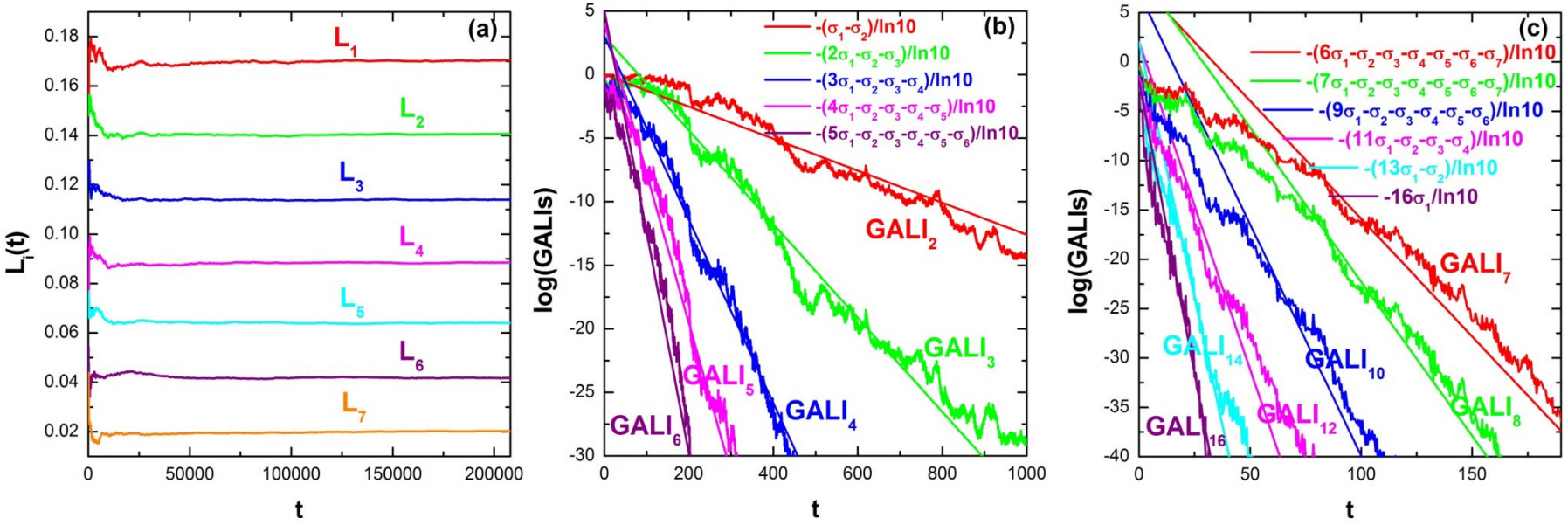

Behavior of $GALI_k$ for regular motion

If the motion occurs on an s-dimensional torus with $s \leq N$ then the behavior of $GALI_k$ is given by (Ch.S., Bountis, Antonopoulos, 2008, Eur. Phys. J. Sp. Top.):

$$GALI_k(t) \propto \begin{cases} \text{constant} & \text{if} \quad 2 \leq k \leq s \\ \dfrac{1}{t^{k-s}} & \text{if} \quad s < k \leq 2N - s \\ \dfrac{1}{t^{2(k-N)}} & \text{if} \quad 2N - s < k \leq 2N \end{cases}$$

while in the common case with $s=N$ we have :

$$GALI_k(t) \propto \begin{cases} \text{constant} & \text{if} \quad 2 \leq k \leq N \\ \dfrac{1}{t^{2(k-N)}} & \text{if} \quad N < k \leq 2N \end{cases}$$

Behavior of $GALI_k$ for regular motion

3D Hamiltonian

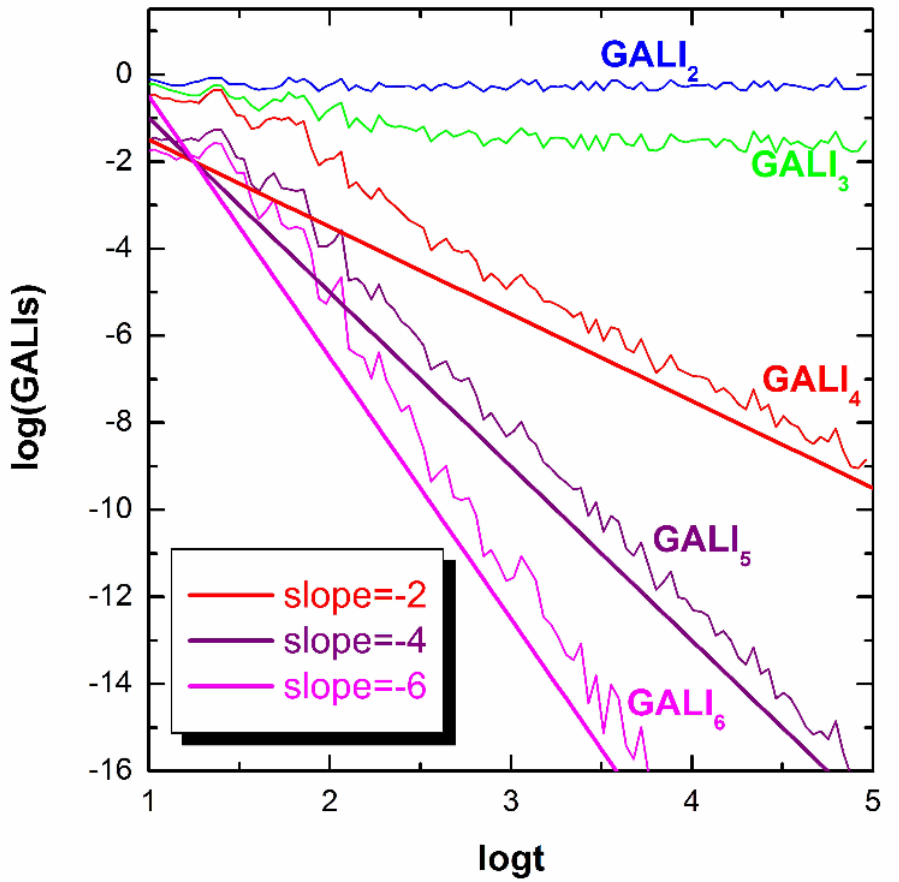

Behavior of $GALI_k$ for regular motion

N=8 FPU system: The unperturbed Hamiltonian (β=0) is written as a sum of the so-called **harmonic energies E_i:**

$$E_i = \frac{1}{2}\left(P_i^2 + \omega_i^2 Q_i^2\right),\ i = 1,...,N$$

with:

$$Q_i = \sqrt{\frac{2}{N+1}}\sum_{k=1}^{N} q_k \sin\left(\frac{ki\pi}{N+1}\right),\ P_i = \sqrt{\frac{2}{N+1}}\sum_{k=1}^{N} p_k \sin\left(\frac{ki\pi}{N+1}\right),\ \omega_i = 2\sin\left(\frac{i\pi}{2(N+1)}\right)$$

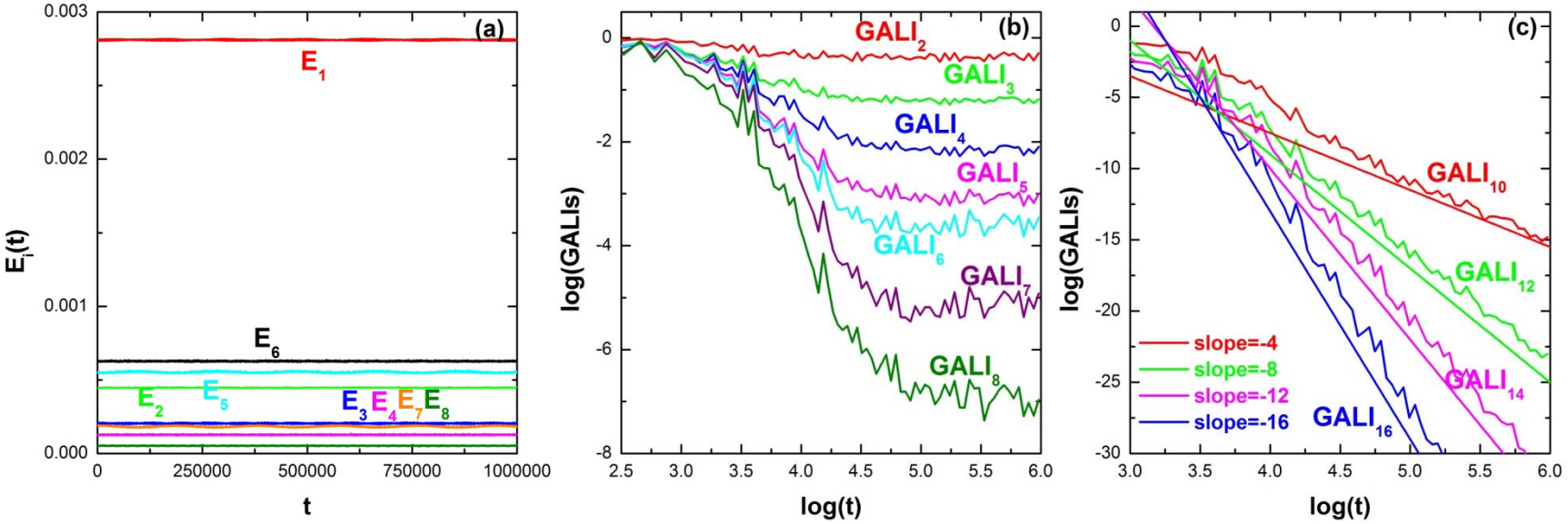

Global dynamics

- $GALI_2$ (practically equivalent to the use of SALI)

- $GALI_N$

Chaotic motion: $GALI_N \to 0$ (exponential decay)

Regular motion: $GALI_N \to$ constant$\neq 0$

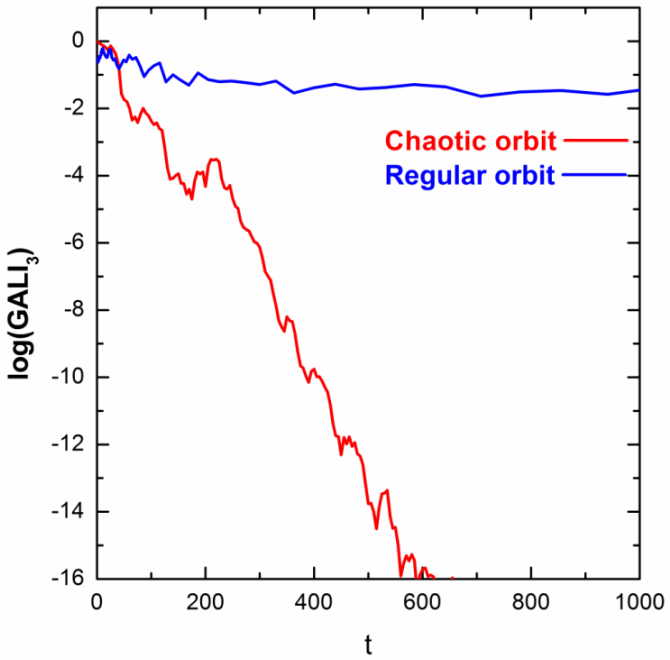

3D Hamiltonian

Subspace $q_3=p_3=0$, $p_2 \geq 0$ for t=1000.

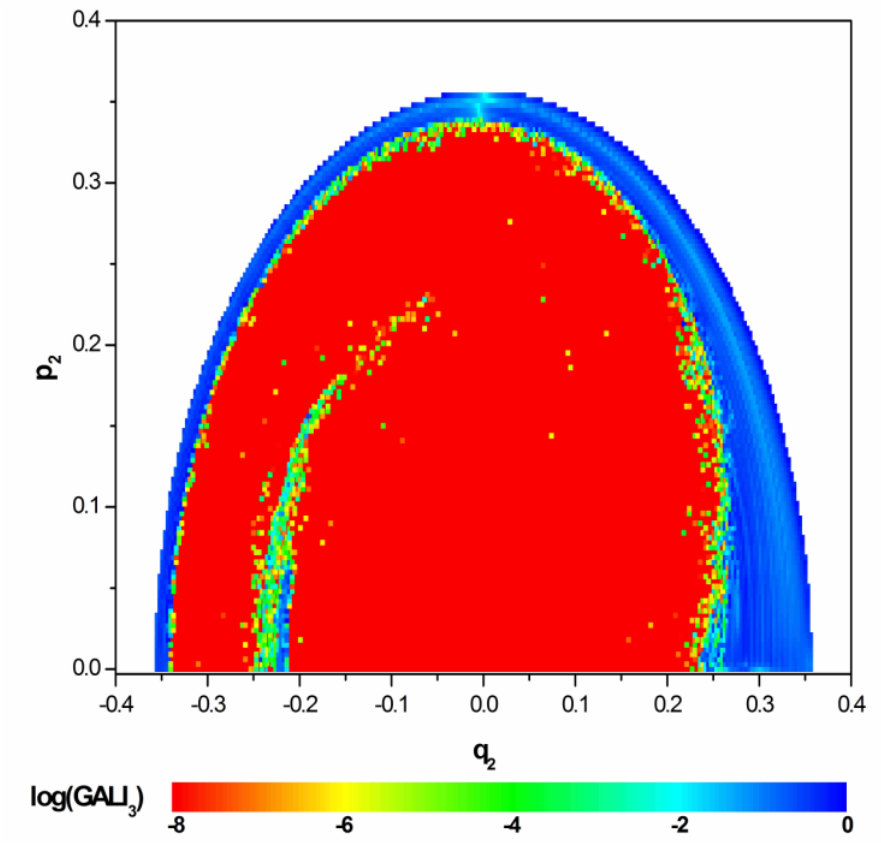

Global dynamics

$GALI_k$ with k>N

The index tends to zero both for regular and chaotic orbits but with completely different time rates:

Chaotic motion: exponential decay

Regular motion: power law

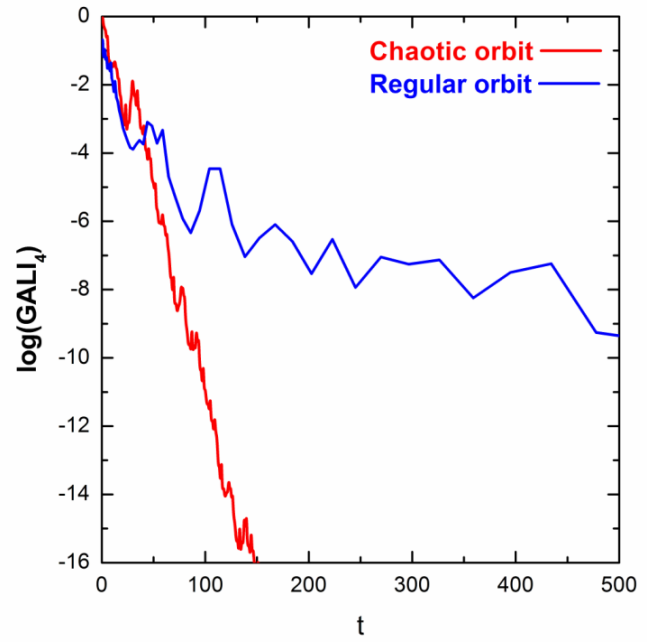

2D Hamiltonian (Hénon-Heiles)
Time needed for $GALI_4<10^{-12}$

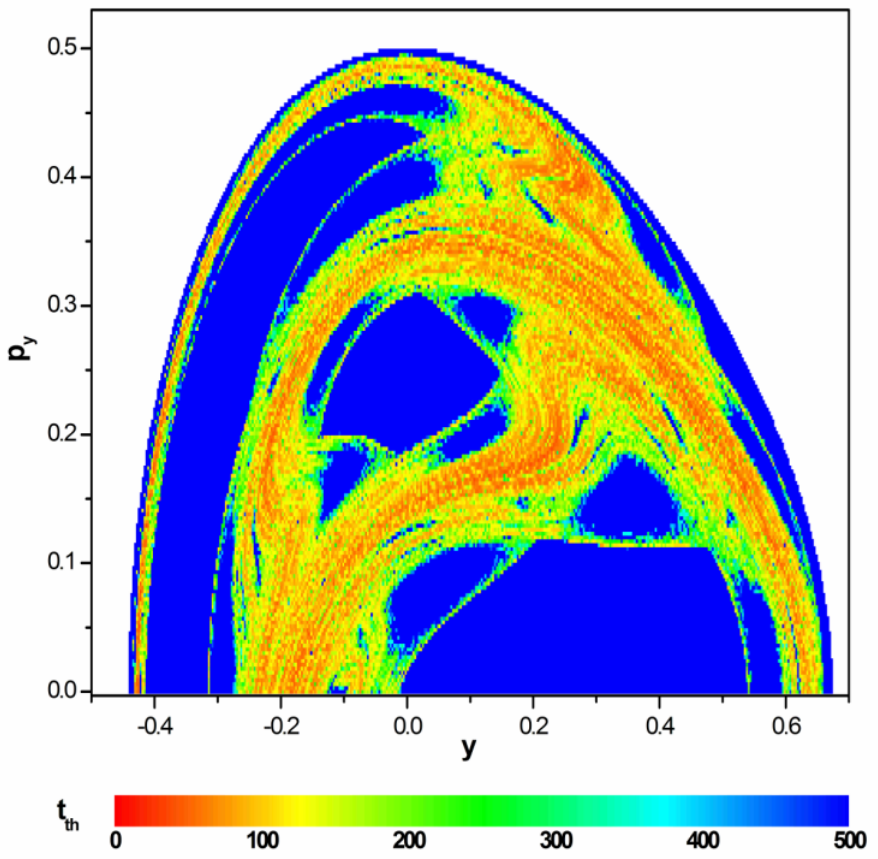

Behavior of $GALI_k$

Chaotic motion:

$GALI_k \to 0$ exponential decay

$$GALI_k(t) \propto e^{-[(\sigma_1-\sigma_2)+(\sigma_1-\sigma_3)+\ldots+(\sigma_1-\sigma_k)]t}$$

Regular motion:

$GALI_k \to$ constant $\neq 0$ or $GALI_k \to 0$ power law decay

$$GALI_k(t) \propto \begin{cases} \text{constant} & \text{if} \quad 2 \le k \le s \\ \dfrac{1}{t^{k-s}} & \text{if} \quad s < k \le 2N-s \\ \dfrac{1}{t^{2(k-N)}} & \text{if} \quad 2N-s < k \le 2N \end{cases}$$

Regular motion on low-dimensional tori

A regular orbit lying on a 2-dimensional torus for the N=8 FPU system.

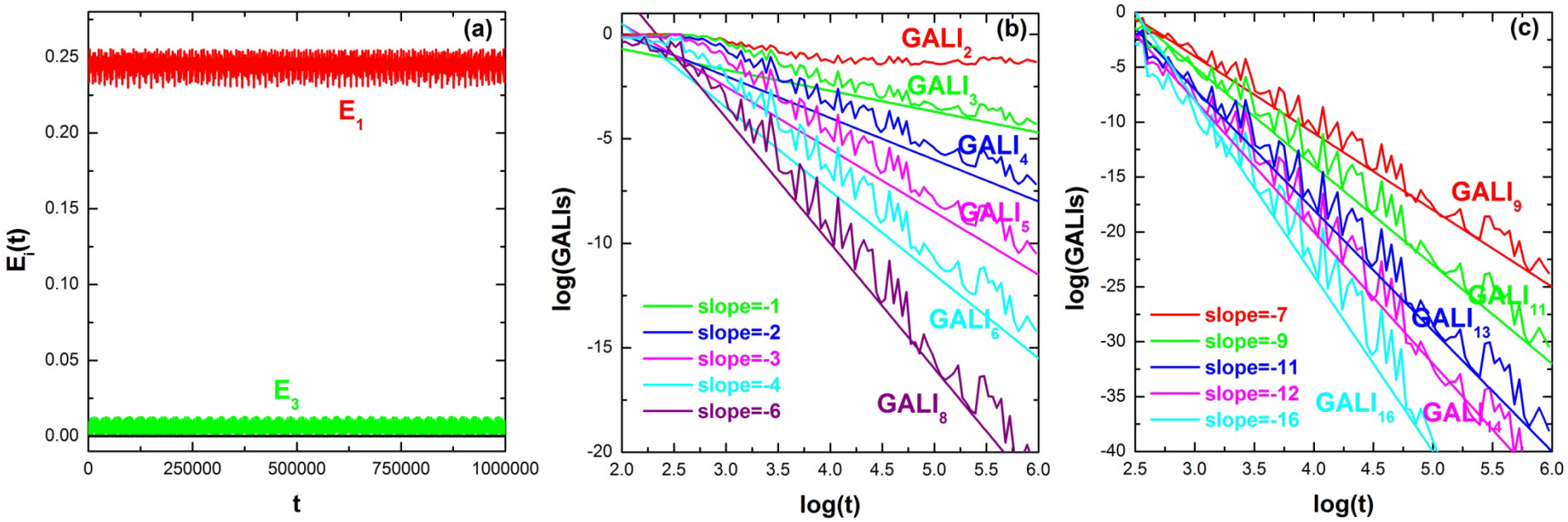

Regular motion on low-dimensional tori

A regular orbit lying on a 4-dimensional torus for the N=8 FPU system.

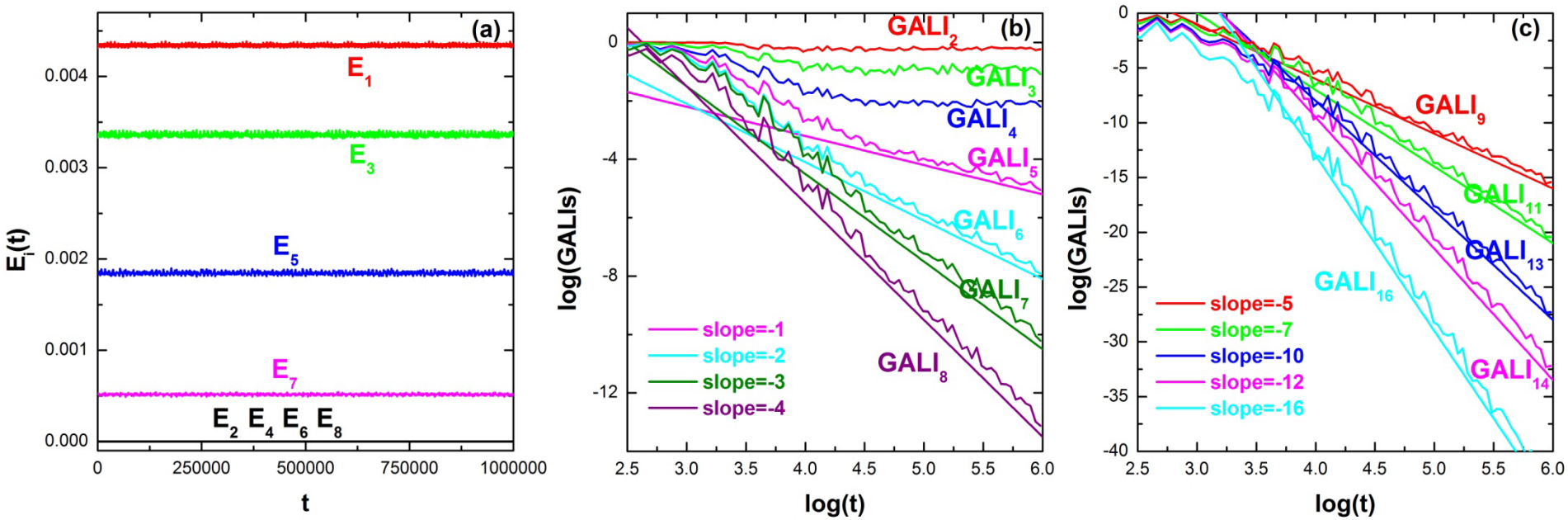

Low-dimensional tori - 6D map

$$
\begin{aligned}
x_1' &= x_1 + x_2' \\
x_2' &= x_2 + \frac{K_1}{2\pi}\sin(2\pi x_1) - \frac{B}{2\pi}\{\sin[2\pi(x_5 - x_1)] + \sin[2\pi(x_3 - x_1)]\} \\
x_3' &= x_3 + x_4' \\
x_4' &= x_4 + \frac{K_2}{2\pi}\sin(2\pi x_3) - \frac{B}{2\pi}\{\sin[2\pi(x_1 - x_3)] + \sin[2\pi(x_5 - x_3)]\} \quad \text{(mod 1)} \\
x_5' &= x_5 + x_6' \\
x_6' &= x_6 + \frac{K_3}{2\pi}\sin(2\pi x_5) - \frac{B}{2\pi}\{\sin[2\pi(x_3 - x_5)] + \sin[2\pi(x_1 - x_5)]\}
\end{aligned}
$$

3D torus

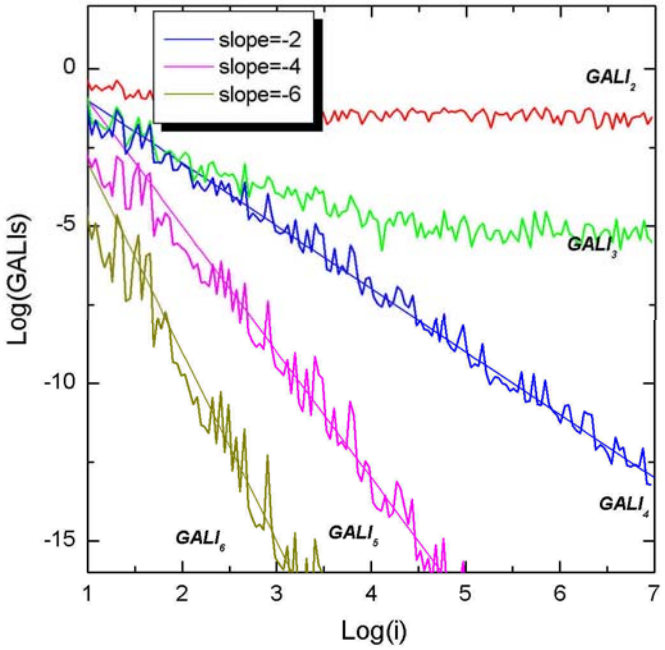

2D torus

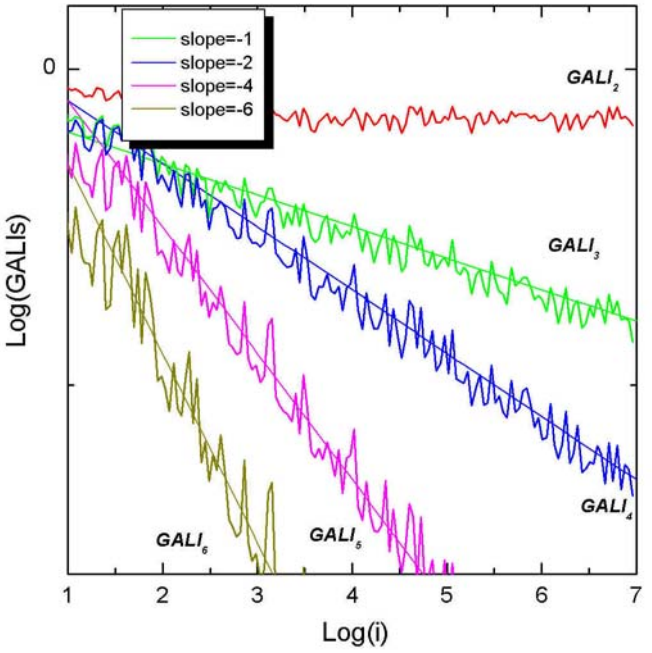

Locating low-dimensional tori

Orbits with $q_1=q_2=0.1$, $p_1=p_2=p_3=0$, H=0.010075 for the N=4 FPU system (Gerlach, Eggl, Ch.S., 2011, nlin.CD/1104.3127).

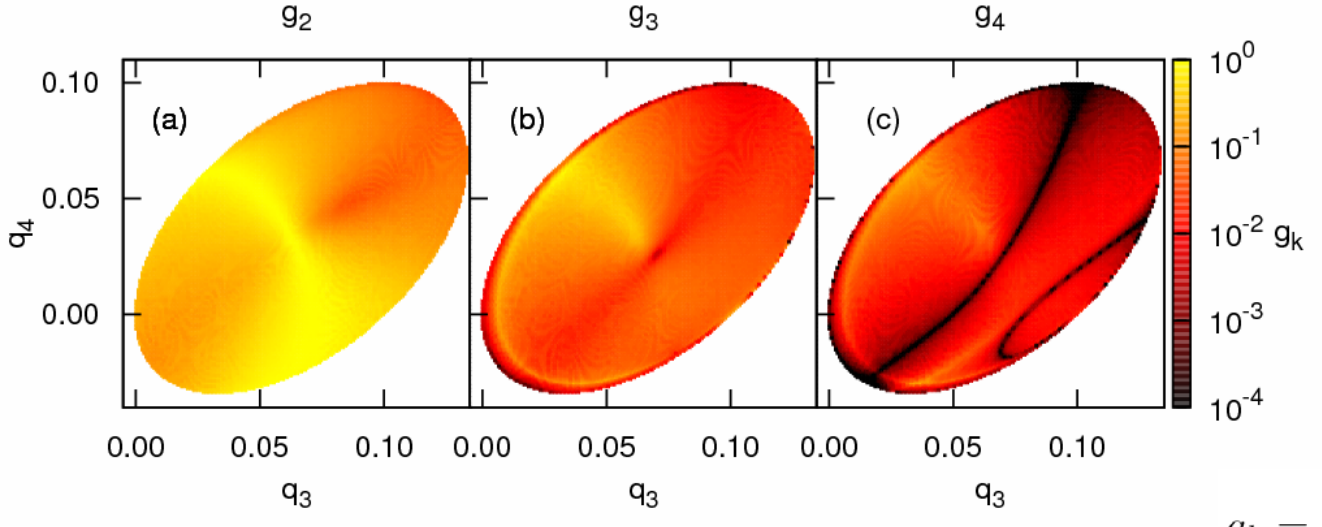

$$g_k = \frac{\mathrm{GALI}_k}{\max(\mathrm{GALI}_k)}$$

Locating low-dimensional tori

Orbits with $q_1=q_2=0.1$, $p_1=p_2=p_3=0$, H=0.010075 for the N=4 FPU system (Gerlach, Eggl, Ch.S., 2011, nlin.CD/1104.3127).

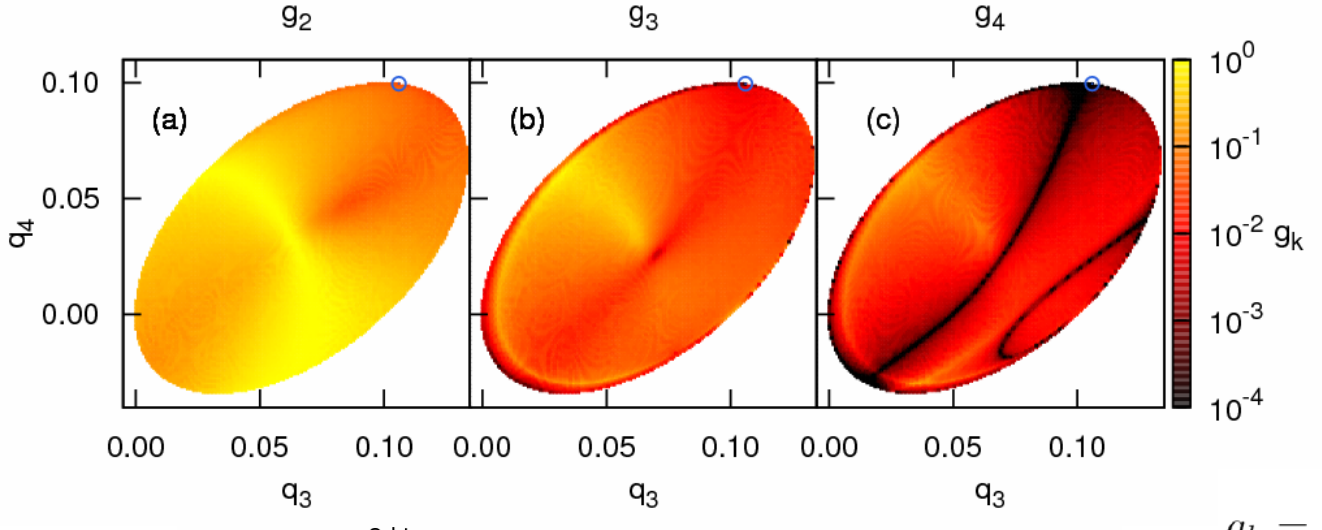

$$g_k = \frac{\mathrm{GALI}_k}{\max(\mathrm{GALI}_k)}$$

2d torus

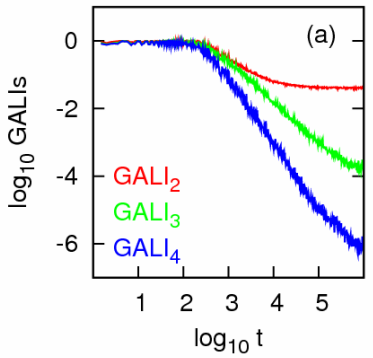

Locating low-dimensional tori

Orbits with $q_1=q_2=0.1$, $p_1=p_2=p_3=0$, H=0.010075 for the N=4 FPU system (Gerlach, Eggl, Ch.S., 2011, nlin.CD/1104.3127).

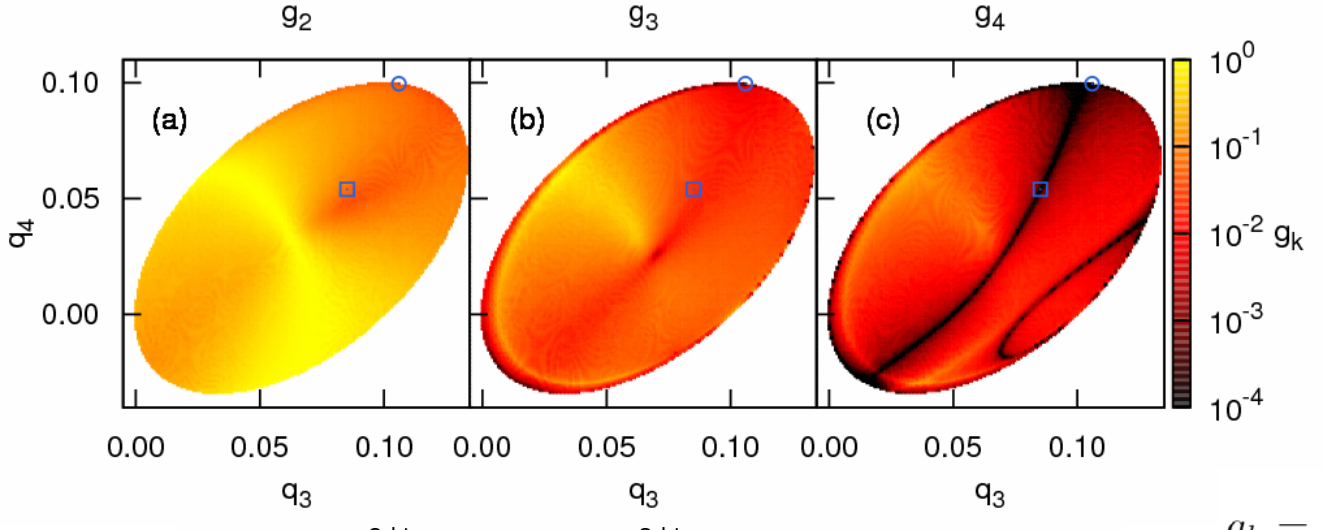

$$g_k = \frac{\mathrm{GALI}_k}{\max(\mathrm{GALI}_k)}$$

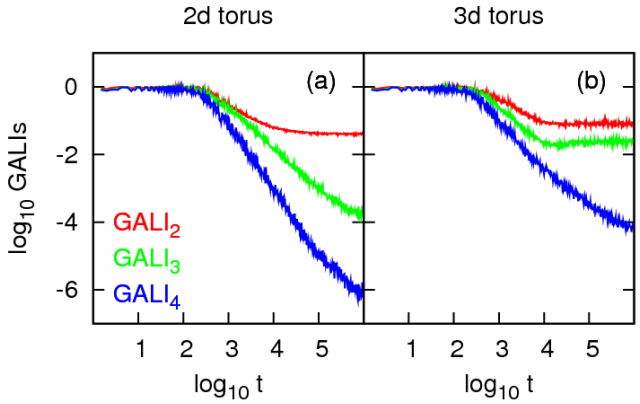

Locating low-dimensional tori

Orbits with $q_1=q_2=0.1$, $p_1=p_2=p_3=0$, H=0.010075 for the N=4 FPU system (Gerlach, Eggl, Ch.S., 2011, nlin.CD/1104.3127).

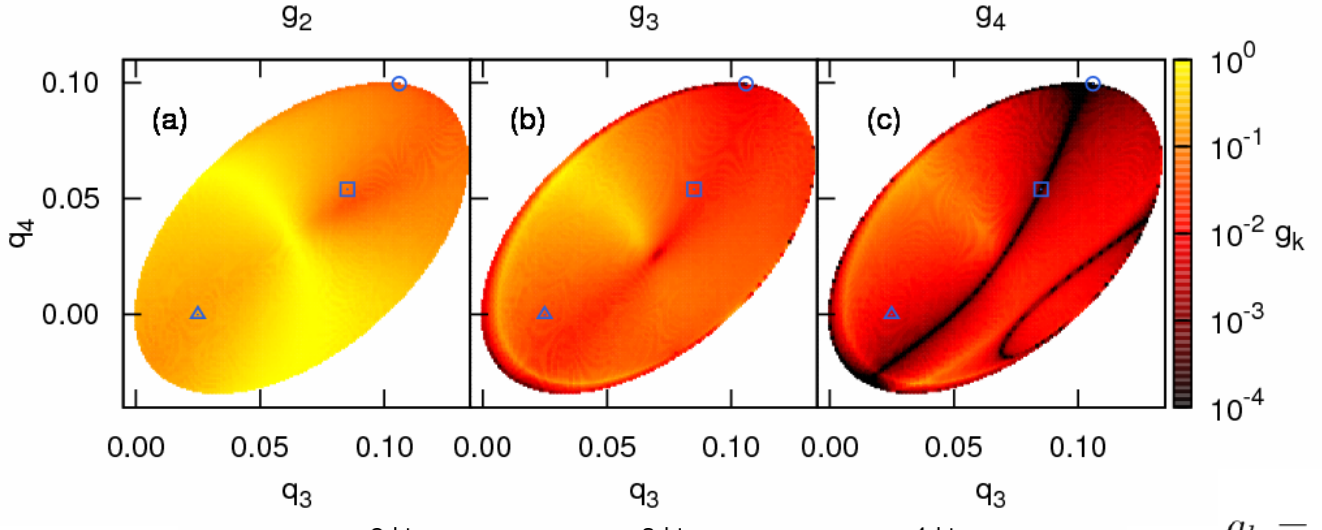

$$g_k = \frac{\mathrm{GALI}_k}{\max(\mathrm{GALI}_k)}$$

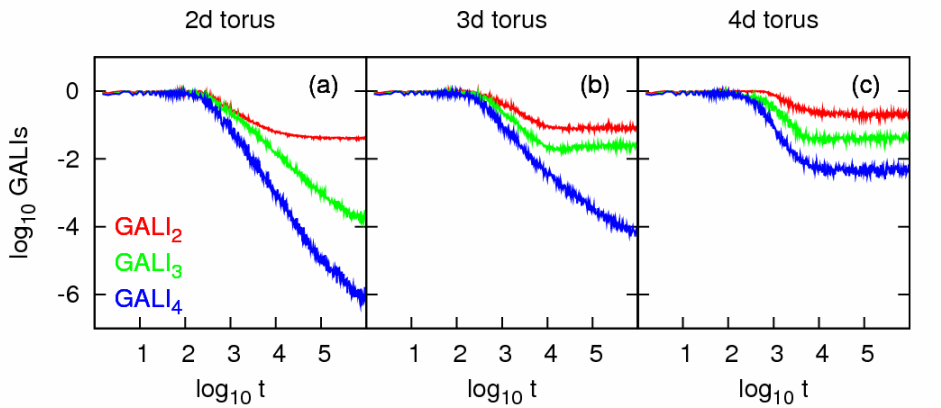

Efficient integration of variational equations

Consider an N degree of freedom autonomous Hamiltonian system having a Hamiltonian function of the form:

$$H(\vec{q},\vec{p}) = \frac{1}{2}\sum_{i=1}^{N} p_i^2 + V(\vec{q})$$

with $\vec{q} = (q_1(t), q_2(t), \ldots, q_N(t))$ $\vec{p} = (p_1(t), p_2(t), \ldots, p_N(t))$ **being respectively the coordinates and momenta.**

The time evolution of an orbit is governed by the Hamilton's equations of motion

$$\dot{\vec{q}} = \vec{p}$$
$$\dot{\vec{p}} = -\frac{\partial V}{\partial \vec{q}}$$

Variational Equations

The time evolution of a deviation vector

$$\vec{w}(t) = (\delta q_1(t), \delta q_2(t), \ldots, \delta q_N(t), \delta p_1(t), \delta p_2(t), \ldots, \delta p_N(t))$$

from a given orbit is governed by the variational equations:

$$\dot{\delta\vec{q}} = \delta\vec{p}$$
$$\dot{\delta\vec{p}} = -\mathbf{D}^2\mathbf{V}(\vec{q}(t))\delta\vec{q}$$

where $$\mathbf{D}^2\mathbf{V}(\vec{q}(t))_{jk} = \left.\frac{\partial^2 V(\vec{q})}{\partial q_j \partial q_k}\right|_{\vec{q}(t)}, \quad j,k = 1,2,\ldots,N.$$

The variational equations are the equations of motion of the time dependent tangent dynamics Hamiltonian (TDH) function

$$H_V(\delta\vec{q}, \delta\vec{p}; t) = \frac{1}{2}\sum_{j=1}^{N} \delta p_i^2 + \frac{1}{2}\sum_{j,k}^{N} \mathbf{D}^2\mathbf{V}(\vec{q}(t))_{jk}\delta q_j \delta q_k$$

Autonomous Hamiltonian systems

As an example, we consider the Hénon-Heiles system:

$$H_2 = \frac{1}{2}(p_x^2 + p_y^2) + \frac{1}{2}(x^2 + y^2) + x^2 y - \frac{1}{3}y^3$$

Hamilton's equations of motion:

$$\begin{cases} \dot{x} &= p_x \\ \dot{y} &= p_y \\ \dot{p}_x &= -x - 2xy \\ \dot{p}_y &= y^2 - x^2 - y \end{cases}$$

Variational equations:

$$\begin{cases} \dot{\delta x} &= \delta p_x \\ \dot{\delta y} &= \delta p_y \\ \dot{\delta p}_x &= -(1 + 2y)\delta x - 2x\delta y \\ \dot{\delta p}_y &= -2x\delta x + (-1 + 2y)\delta y \end{cases}$$

Integration of the variational equations

We use two general-purpose numerical integration algorithms for the integration of the whole set of equations:

$$\begin{cases} \dot{x} &= p_x \\ \dot{y} &= p_y \\ \dot{p}_x &= -x - 2xy \\ \dot{p}_y &= y^2 - x^2 - y \\ \dot{\delta x} &= \delta p_x \\ \dot{\delta y} &= \delta p_y \\ \dot{\delta p}_x &= -(1+2y)\delta x - 2x\delta y \\ \dot{\delta p}_y &= -2x\delta x + (-1+2y)\delta y \end{cases}$$

a) the DOP853 integrator (Hairer et al. 1993, http://www.unige.ch/~hairer/software.html), which is an explicit non-symplectic Runge-Kutta integration scheme of order 8,

b) the TIDES integrator (Barrio 2005, http://gme.unizar.es/software/tides), which is based on a Taylor series approximation

$$\boldsymbol{y}(t_i+\tau) \simeq \boldsymbol{y}(t_i) + \tau\frac{\mathrm{d}\boldsymbol{y}(t_i)}{\mathrm{d}t} + \frac{\tau^2}{2!}\frac{\mathrm{d}^2\boldsymbol{y}(t_i)}{\mathrm{d}t^2} + \ldots + \frac{\tau^n}{n!}\frac{\mathrm{d}^n\boldsymbol{y}(t_i)}{\mathrm{d}t^n}$$

for the solution of system

$$\frac{\mathrm{d}\boldsymbol{y}(t)}{\mathrm{d}t} = \boldsymbol{f}(\boldsymbol{y}(t))$$

Symplectic Integration schemes

Formally the solution of the Hamilton's equations of motion can be written as:

$$\frac{d\vec{X}}{dt} = \left\{H, \vec{X}\right\} = L_H \vec{X} \Rightarrow \vec{X}(t) = \sum_{n\geq 0} \frac{t^n}{n!} L_H^n \vec{X} = e^{tL_H} \vec{X}$$

where $\vec{X}$ is the full coordinate vector and L_H the Poisson operator:

$$L_H f = \sum_{j=1}^{N} \left\{ \frac{\partial H}{\partial p_j}\frac{\partial f}{\partial q_j} - \frac{\partial H}{\partial q_j}\frac{\partial f}{\partial p_j} \right\}$$

If the Hamiltonian H can be split into two integrable parts as H=A+B, a symplectic scheme for integrating the equations of motion from time t to time t+τ consists of approximating the operator $e^{\tau L_H}$ by

$$e^{\tau L_H} = e^{\tau(L_A + L_B)} \approx \prod_{i=1}^{j} e^{c_i \tau L_A} e^{d_i \tau L_B}$$

for appropriate values of constants c_i, d_i.

So the dynamics over an integration time step τ is described by a series of successive acts of Hamiltonians A and B.

Symplectic Integrator $SABA_2C$

We use a symplectic integration scheme developed for Hamiltonians of the form $H=A+\varepsilon B$ where A, B are both integrable and ε a parameter. The operator $e^{\tau L_H}$ can be approximated by the symplectic integrator (Laskar & Robutel, 2001, Cel. Mech. Dyn. Astr.):

$$SABA_2 = e^{c_1 \tau L_A}\ e^{d_1 \tau L_{\varepsilon B}}\ e^{c_2 \tau L_A}\ e^{d_1 \tau L_{\varepsilon B}}\ e^{c_1 \tau L_A}$$

with $c_1 = \frac{(3-\sqrt{3})}{6}$, $c_2 = \frac{\sqrt{3}}{3}$, $d_1 = \frac{1}{2}$.

The integrator has only positive steps and its error is of order $O(\tau^4\varepsilon+\tau^2\varepsilon^2)$.

In the case where A is quadratic in the momenta and B depends only on the positions the method can be improved by introducing a corrector $C=\{\{A,B\},B\}$, having a small negative step: $e^{-\tau^3\varepsilon^2 \frac{c}{2} L_{\{\{A,B\},B\}}}$

with $c = \frac{(2-\sqrt{3})}{24}$.

Thus the full integrator scheme becomes: $SABAC_2 = C\ (SABA_2)\ C$ and its error is of order $O(\tau^4\varepsilon+\tau^4\varepsilon^2)$.

Tangent Map (TM) Method

Use symplectic integration schemes for the whole set of equations (Ch.S., Gerlach, 2010, PRE)

We apply the $SABAC_2$ integrator scheme to the Hénon-Heiles system (with ε=1) by using the splitting:

$$A = \frac{1}{2}(p_x^2 + p_y^2), \qquad B = \frac{1}{2}(x^2 + y^2) + x^2 y - \frac{1}{3}y^3,$$

with a corrector term which corresponds to the Hamiltonian function:

$$C = \{\{A, B\}, B\} = (x + 2xy)^2 + \left(x^2 - y^2 + y\right)^2$$

We approximate the dynamics by the act of Hamiltonians A, B and C, which correspond to the symplectic maps:

$$e^{\tau L_A} : \begin{cases} x' &= x + p_x\tau \\ y' &= y + p_y\tau \\ p_x' &= p_x \\ p_y' &= p_y \end{cases},$$

$$e^{\tau L_B} : \begin{cases} x' &= x \\ y' &= y \\ p_x' &= p_x - x(1+2y)\tau \\ p_y' &= p_y + (y^2 - x^2 - y)\tau \end{cases},$$

$$e^{\tau L_C} : \begin{cases} x' &= x \\ y' &= y \\ p_x' &= p_x - 2x(1 + 2x^2 + 6y + 2y^2)\tau \\ p_y' &= p_y - 2(y - 3y^2 + 2y^3 + 3x^2 + 2x^2 y)\tau \end{cases}.$$

Tangent Map (TM) Method

Let $\vec{u} = (x, y, p_x, p_y, \delta x, \delta y, \delta p_x, \delta p_y)$

The system of the Hamilton's equations of motion and the variational equations is split into two integrable systems which correspond to Hamiltonians A and B.

$$
\begin{aligned}
\dot{x} &= p_x \\
\dot{y} &= p_y \\
\dot{p}_x &= -x - 2xy \\
\dot{p}_y &= y^2 - x^2 - y
\end{aligned}
$$

$$
\begin{aligned}
\dot{\delta x} &= \delta p_x \\
\dot{\delta y} &= \delta p_y \\
\dot{\delta p}_x &= -(1+2y)\delta x - 2x\delta y \\
\dot{\delta p}_y &= -2x\delta x + (-1+2y)\delta y
\end{aligned}
$$

Tangent Map (TM) Method

Let $\vec{u} = (x, y, p_x, p_y, \delta x, \delta y, \delta p_x, \delta p_y)$

The system of the Hamilton's equations of motion and the variational equations is split into two integrable systems which correspond to Hamiltonians A and B.

$$\begin{aligned}
\dot{x} &= p_x \\
\dot{y} &= p_y \\
\dot{p}_x &= -x - 2xy \\
\dot{p}_y &= y^2 - x^2 - y \\
\dot{\delta x} &= \delta p_x \\
\dot{\delta y} &= \delta p_y \\
\dot{\delta p}_x &= -(1+2y)\delta x - 2x\delta y \\
\dot{\delta p}_y &= -2x\delta x + (-1+2y)\delta y
\end{aligned}
\xrightarrow{A(\vec{p})}
\left.\begin{aligned}
\dot{x} &= p_x \\
\dot{y} &= p_y \\
\dot{p}_x &= 0 \\
\dot{p}_y &= 0 \\
\dot{\delta x} &= \delta p_x \\
\dot{\delta y} &= \delta p_y \\
\dot{\delta p}_x &= 0 \\
\dot{\delta p}_y &= 0
\end{aligned}\right\} \Rightarrow \frac{d\vec{u}}{dt} = L_{AV}\vec{u}$$

Tangent Map (TM) Method

Let $\vec{u} = (x, y, p_x, p_y, \delta x, \delta y, \delta p_x, \delta p_y)$

The system of the Hamilton's equations of motion and the variational equations is split into two integrable systems which correspond to Hamiltonians A and B.

$$\left.\begin{aligned}
\dot{x} &= p_x \\
\dot{y} &= p_y \\
\dot{p}_x &= -x - 2xy \\
\dot{p}_y &= y^2 - x^2 - y \\
\dot{\delta x} &= \delta p_x \\
\dot{\delta y} &= \delta p_y \\
\dot{\delta p}_x &= -(1+2y)\delta x - 2x\delta y \\
\dot{\delta p}_y &= -2x\delta x + (-1+2y)\delta y
\end{aligned}\right\} \xrightarrow{A(\vec{p})} \left.\begin{aligned}
\dot{x} &= p_x \\
\dot{y} &= p_y \\
\dot{p}_x &= 0 \\
\dot{p}_y &= 0 \\
\dot{\delta x} &= \delta p_x \\
\dot{\delta y} &= \delta p_y \\
\dot{\delta p}_x &= 0 \\
\dot{\delta p}_y &= 0
\end{aligned}\right\} \Rightarrow \frac{d\vec{u}}{dt} = L_{AV}\vec{u}$$

$$B(\vec{q}) \left\{\begin{aligned}
\dot{x} &= 0 \\
\dot{y} &= 0 \\
\dot{p}_x &= -x - 2xy \\
\dot{p}_y &= y^2 - x^2 - y \\
\dot{\delta x} &= 0 \\
\dot{\delta y} &= 0 \\
\dot{\delta p}_x &= -(1+2y)\delta x - 2x\delta y \\
\dot{\delta p}_y &= -2x\delta x + (-1+2y)\delta y
\end{aligned}\right. \Rightarrow \frac{d\vec{u}}{dt} = L_{BV}\vec{u}$$

Tangent Map (TM) Method

Let $\vec{u} = (x, y, p_x, p_y, \delta x, \delta y, \delta p_x, \delta p_y)$

The system of the Hamilton's equations of motion and the variational equations is split into two integrable systems which correspond to Hamiltonians A and B.

$$\begin{aligned}
\dot{x} &= p_x \\
\dot{y} &= p_y \\
\dot{p}_x &= -x - 2xy \\
\dot{p}_y &= y^2 - x^2 - y \\
\dot{\delta x} &= \delta p_x \\
\dot{\delta y} &= \delta p_y \\
\dot{\delta p}_x &= -(1+2y)\delta x - 2x\delta y \\
\dot{\delta p}_y &= -2x\delta x + (-1+2y)\delta y
\end{aligned}$$

$A(\vec{p})$

$$\left.\begin{aligned}
\dot{x} &= p_x \\
\dot{y} &= p_y \\
\dot{p}_x &= 0 \\
\dot{p}_y &= 0 \\
\dot{\delta x} &= \delta p_x \\
\dot{\delta y} &= \delta p_y \\
\dot{\delta p}_x &= 0 \\
\dot{\delta p}_y &= 0
\end{aligned}\right\} \Rightarrow \frac{d\vec{u}}{dt} = L_{AV}\vec{u} \Rightarrow e^{\tau L_{AV}} : \left\{\begin{aligned}
x' &= x + p_x\tau \\
y' &= y + p_y\tau \\
px' &= p_x \\
py' &= p_y \\
\delta x' &= \delta x + \delta p_x\tau \\
\delta y' &= \delta y + \delta p_y\tau \\
\delta p_x' &= \delta p_x \\
\delta p_y' &= \delta p_y
\end{aligned}\right.$$

$B(\vec{q})$

$$\left.\begin{aligned}
\dot{x} &= 0 \\
\dot{y} &= 0 \\
\dot{p}_x &= -x - 2xy \\
\dot{p}_y &= y^2 - x^2 - y \\
\dot{\delta x} &= 0 \\
\dot{\delta y} &= 0 \\
\dot{\delta p}_x &= -(1+2y)\delta x - 2x\delta y \\
\dot{\delta p}_y &= -2x\delta x + (-1+2y)\delta y
\end{aligned}\right\} \Rightarrow \frac{d\vec{u}}{dt} = L_{BV}\vec{u} \Rightarrow e^{\tau L_{BV}} : \left\{\begin{aligned}
x' &= x \\
y' &= y \\
p_x' &= p_x - x(1+2y)\tau \\
p_y' &= p_y + (y^2 - x^2 - y)\tau \\
\delta x' &= \delta x \\
\delta y' &= \delta y \\
\delta p_x' &= \delta p_x - [(1+2y)\delta x + 2x\delta y]\,\tau \\
\delta p_y' &= \delta p_y + [-2x\delta x + (-1+2y)\delta y]\,\tau
\end{aligned}\right.$$

Tangent Map (TM) Method

So any symplectic integration scheme used for solving the Hamilton's equations of motion, which involves the act of Hamiltonians A, B and C, can be extended in order to integrate simultaneously the variational equations.

$$e^{\tau L_A} : \begin{cases} x' &= x + p_x \tau \\ y' &= y + p_y \tau \\ p_x' &= p_x \\ p_y' &= p_y \end{cases}$$

$$e^{\tau L_B} : \begin{cases} x' &= x \\ y' &= y \\ p_x' &= p_x - x(1+2y)\tau \\ p_y' &= p_y + (y^2 - x^2 - y)\tau \end{cases}$$

$$e^{\tau L_C} : \begin{cases} x' &= x \\ y' &= y \\ p_x' &= p_x - 2x(1 + 2x^2 + 6y + 2y^2)\tau \\ p_y' &= p_y - 2(y - 3y^2 + 2y^3 + 3x^2 + 2x^2 y)\tau \end{cases}$$

Tangent Map (TM) Method

So any symplectic integration scheme used for solving the Hamilton's equations of motion, which involves the act of Hamiltonians A, B and C, can be extended in order to integrate simultaneously the variational equations.

$$e^{\tau L_A}: \begin{cases} x' &= x + p_x\tau \\ y' &= y + p_y\tau \\ p_x' &= p_x \\ p_y' &= p_y \end{cases} \rightarrow e^{\tau L_{AV}}: \begin{cases} x' &= x + p_x\tau \\ y' &= y + p_y\tau \\ px' &= p_x \\ py' &= p_y \\ \delta x' &= \delta x + \delta p_x\tau \\ \delta y' &= \delta y + \delta p_y\tau \\ \delta p_x' &= \delta p_x \\ \delta p_y' &= \delta p_y \end{cases}$$

$$e^{\tau L_B}: \begin{cases} x' &= x \\ y' &= y \\ p_x' &= p_x - x(1+2y)\tau \\ p_y' &= p_y + (y^2 - x^2 - y)\tau \end{cases}$$

$$e^{\tau L_C}: \begin{cases} x' &= x \\ y' &= y \\ p_x' &= p_x - 2x(1 + 2x^2 + 6y + 2y^2)\tau \\ p_y' &= p_y - 2(y - 3y^2 + 2y^3 + 3x^2 + 2x^2y)\tau \end{cases}$$

Tangent Map (TM) Method

So any symplectic integration scheme used for solving the Hamilton's equations of motion, which involves the act of Hamiltonians A, B and C, can be extended in order to integrate simultaneously the variational equations.

$$e^{\tau L_A}: \begin{cases} x' &= x + p_x\tau \\ y' &= y + p_y\tau \\ p_x' &= p_x \\ p_y' &= p_y \end{cases} \rightarrow e^{\tau L_{AV}}: \begin{cases} x' &= x + p_x\tau \\ y' &= y + p_y\tau \\ px' &= p_x \\ py' &= p_y \\ \delta x' &= \delta x + \delta p_x\tau \\ \delta y' &= \delta y + \delta p_y\tau \\ \delta p_x' &= \delta p_x \\ \delta p_y' &= \delta p_y \end{cases}$$

$$e^{\tau L_B}: \begin{cases} x' &= x \\ y' &= y \\ p_x' &= p_x - x(1+2y)\tau \\ p_y' &= p_y + (y^2 - x^2 - y)\tau \end{cases} \rightarrow e^{\tau L_{BV}}: \begin{cases} x' &= x \\ y' &= y \\ p_x' &= p_x - x(1+2y)\tau \\ p_y' &= p_y + (y^2 - x^2 - y)\tau \\ \delta x' &= \delta x \\ \delta y' &= \delta y \\ \delta p_x' &= \delta p_x - [(1+2y)\delta x + 2x\delta y]\,\tau \\ \delta p_y' &= \delta p_y + [-2x\delta x + (-1+2y)\delta y]\,\tau \end{cases}$$

$$e^{\tau L_C}: \begin{cases} x' &= x \\ y' &= y \\ p_x' &= p_x - 2x(1 + 2x^2 + 6y + 2y^2)\tau \\ p_y' &= p_y - 2(y - 3y^2 + 2y^3 + 3x^2 + 2x^2y)\tau \end{cases}$$

Tangent Map (TM) Method

So any symplectic integration scheme used for solving the Hamilton's equations of motion, which involves the act of Hamiltonians A, B and C, can be extended in order to integrate simultaneously the variational equations.

$$e^{\tau L_A}: \begin{cases} x' &= x + p_x\tau \\ y' &= y + p_y\tau \\ p_x' &= p_x \\ p_y' &= p_y \end{cases} \rightarrow e^{\tau L_{AV}}: \begin{cases} x' &= x + p_x\tau \\ y' &= y + p_y\tau \\ px' &= p_x \\ py' &= p_y \\ \delta x' &= \delta x + \delta p_x\tau \\ \delta y' &= \delta y + \delta p_y\tau \\ \delta p_x' &= \delta p_x \\ \delta p_y' &= \delta p_y \end{cases}$$

$$e^{\tau L_B}: \begin{cases} x' &= x \\ y' &= y \\ p_x' &= p_x - x(1+2y)\tau \\ p_y' &= p_y + (y^2 - x^2 - y)\tau \end{cases} \rightarrow e^{\tau L_{BV}}: \begin{cases} x' &= x \\ y' &= y \\ p_x' &= p_x - x(1+2y)\tau \\ p_y' &= p_y + (y^2 - x^2 - y)\tau \\ \delta x' &= \delta x \\ \delta y' &= \delta y \\ \delta p_x' &= \delta p_x - [(1+2y)\delta x + 2x\delta y]\,\tau \\ \delta p_y' &= \delta p_y + [-2x\delta x + (-1+2y)\delta y]\,\tau \end{cases}$$

$$e^{\tau L_C}: \begin{cases} x' &= x \\ y' &= y \\ p_x' &= p_x - 2x(1+2x^2+6y+2y^2)\tau \\ p_y' &= p_y - 2(y-3y^2+2y^3+3x^2+2x^2y)\tau \end{cases} \rightarrow e^{\tau L_{CV}}: \begin{cases} x' &= x \\ y' &= y \\ p_x' &= p_x - 2x(1+2x^2+6y+2y^2)\tau \\ p_y' &= p_y - 2(y-3y^2+2y^3+3x^2+2x^2y)\tau \\ \delta x' &= \delta x \\ \delta y' &= \delta y \\ \delta p_x' &= \delta p_x - 2\left[(1+6x^2+2y^2+6y)\delta x + \right. \\ & \quad \left. +2x(3+2y)\delta y\right]\tau \\ \delta p_y' &= \delta p_y - 2\left[2x(3+2y)\delta x + \right. \\ & \quad \left. +(1+2x^2+6y^2-6y)\delta y\right]\tau \end{cases}$$

Application: FPU system

N particles Fermi-Pasta-Ulam (FPU) system:

$$H = \frac{1}{2}\sum_{i=1}^{N} p_i^2 + \sum_{i=0}^{N}\left[\frac{1}{2}(q_{i+1} - q_i)^2 + \frac{\beta}{4}(q_{i+1} - q_i)^4\right]$$

with fixed boundary conditions, β=1.5 and N=4 - 20.

N=4. Regular motion on 2d torus. Final time $t=10^6$.

CPU times ≈ 9 s 54 s 1m 37s

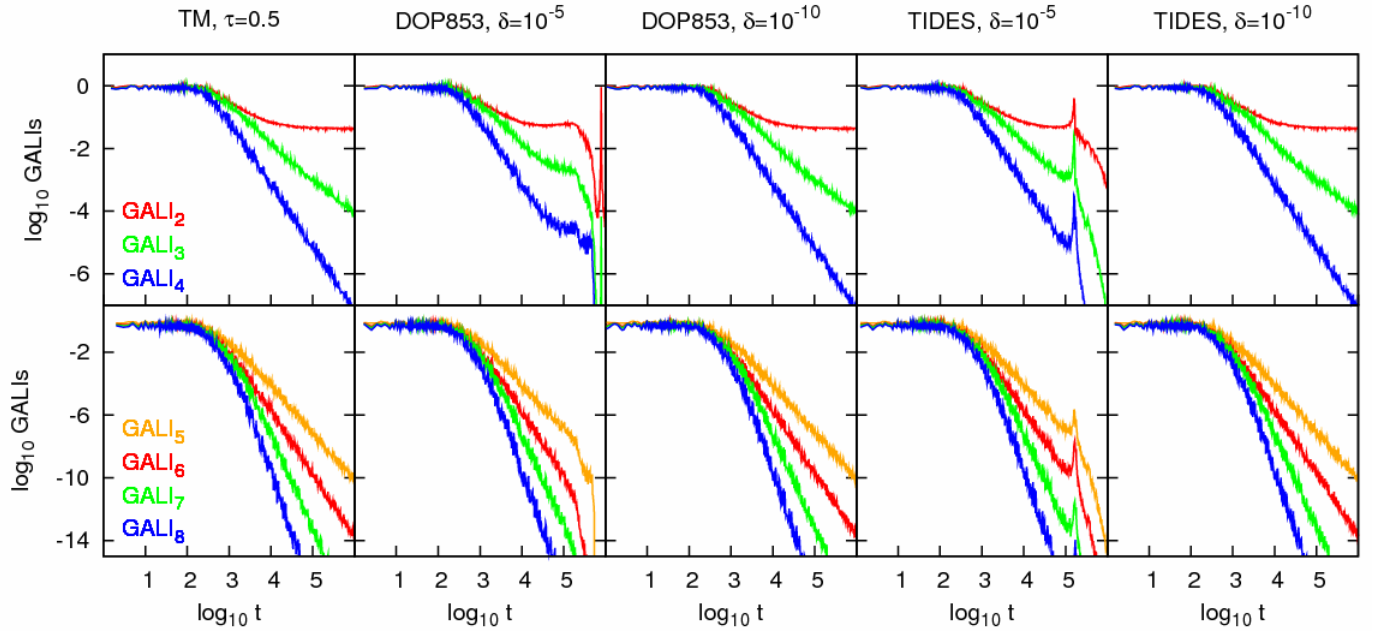

Application: FPU system

N=12. Regular motion on 6d torus. Final time $t=10^8$.

CPU times ≈ **8 h** **22,5 h** **38 h**

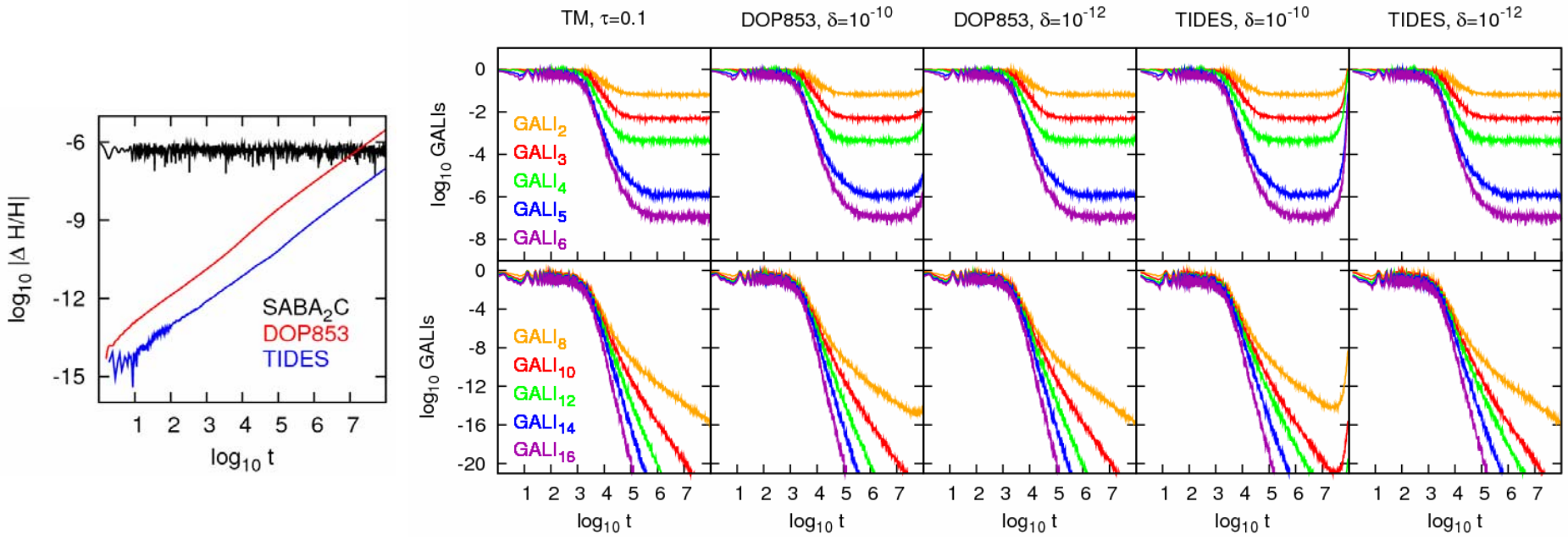

Application: FPU system

Efficiency of different algorithms

Final time $t=10^6$.

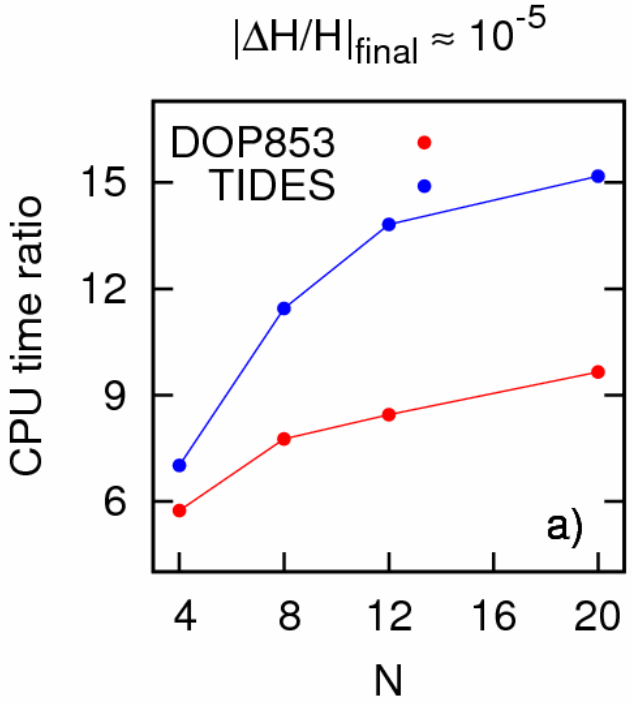

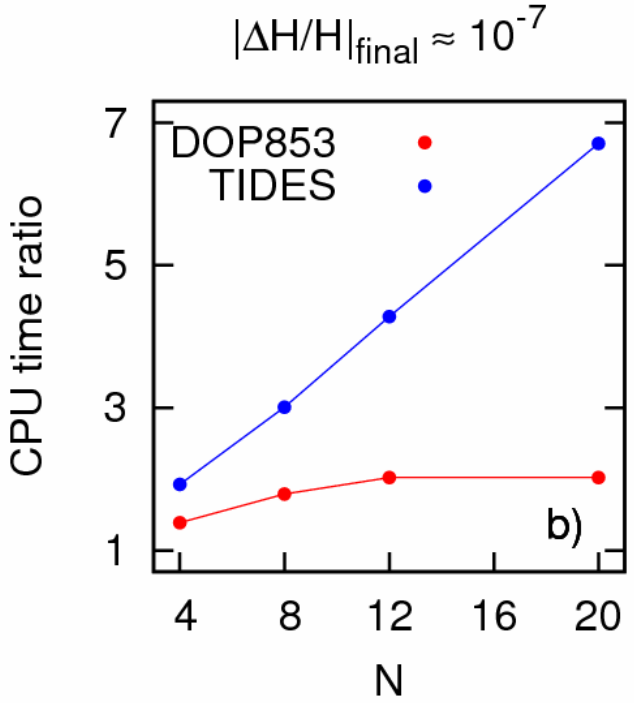

DOP853 $\delta=10^{-10}$

TIDES $\delta=10^{-8}$

SABA$_2$C $\tau=0.5$

DOP853 $\delta=10^{-11}$

TIDES $\delta=10^{-10}$

SABA$_2$C $\tau=0.1$

Conclusions I

- **Generalizing the SALI method we define the Generalized ALignment Index of order k ($GALI_k$) as the volume of the generalized parallelepiped, whose edges are k unit deviation vectors. $GALI_k$ is computed as the product of the singular values of a matrix (SVD algorithm).**

- **Behaviour of $GALI_k$:**
  - ✓ **Chaotic motion: it tends exponentially to zero with exponents that involve the values of several Lyapunov exponents.**
  - ✓ **Regular motion: it fluctuates around non-zero values for $2 \leq k \leq s$ and goes to zero for $s < k \leq 2N$ following power-laws, with s being the dimensionality of the torus.**

Conclusions II

- **$GALI_k$ indices :**
  - ✓ **can distinguish rapidly and with certainty between regular and chaotic motion**
  - ✓ **can be used to characterize individual orbits as well as "chart" chaotic and regular domains in phase space.**
  - ✓ **are perfectly suited for studying the global dynamics of multidimentonal systems**
  - ✓ **can identify regular motion on low–dimensional tori**

- **SALI/GALI methods have been successfully applied to a variety of conservative dynamical systems of**
  - ✓ **Celestial Mechanics (e.g. Széll et al., 2004, MNRAS - Soulis et al., 2008, Cel. Mech. Dyn. Astr. - Libert et al., 2011, MNRAS)**
  - ✓ **Galactic Dynamics (e.g. Capuzzo-Dolcetta et al., 2007, Astroph. J. - Carpintero, 2008, MNRAS - Manos & Athanassoula, 2011, MNRAS, in press)**
  - ✓ **Nuclear Physics (e.g. Macek et al., 2007, Phys. Rev. C - Stránský et al., 2007, Phys. Atom. Nucl. - Stránský et al., 2009, Phys. Rev. E)**
  - ✓ **Statistical Physics (e.g. Manos & Ruffo, 2010, nlin.CD/1006.5341)**

Conclusions III

- **Tangent map (TM) method: Symplectic integrators can be used for the efficient integration of the Hamilton's equations of motion and the variational equations.**
  - ✓ **They reproduce accurately the properties of chaos indicators like the GALIs.**
  - ✓ **These algorithms have better performance than non-symplectic schemes in CPU time requirements. This characteristic is of great importance especially for multidimensional systems.**

Main references

- **SALI**
  - ✓ Ch.S. (2001) J. Phys. A, 34, 10029
  - ✓ Ch.S., Antonopoulos Ch., Bountis T. C. & Vrahatis M. N. (2003) Prog. Theor. Phys. Supp., 150, 439
  - ✓ Ch.S., Antonopoulos Ch., Bountis T. C. & Vrahatis M. N. (2004) J. Phys. A, 37, 6269

- **GALI**
  - ✓ Ch.S., Bountis T. C. & Antonopoulos Ch. (2007) Physica D, 231, 30-54
  - ✓ Ch.S., Bountis T. C. & Antonopoulos Ch. (2008) Eur. Phys. J. Sp. Top., 165, 5-14
  - ✓ Manos T., Ch.S. & Antonopoulos Ch. (2011) arXiv:nlin.CD/1103.0700

- **TM method**
  - ✓ Ch.S. & Gerlach E. (2010) Phys. Rev. E, 82, 036704
  - ✓ Gerlach E. & Ch.S. (2011) In press: 8th AIMS International Conference, arXiv:nlin.CD/1008.1890
  - ✓ Gerlach E., Eggl S. & Ch.S. (2011) arXiv:nlin.CD/1104.3127